

**Synthesis of 3D Flexible Electrode of Hybrid Supercapacitor  
Derived from Biomass via In-Situ Polymerization of  
Polyaniline a Conducting Polymer**



*By*

Saman Anwar

CIIT/SP22-RPH-005/LHR

MS Thesis

In

MS Physics

COMSATS University Islamabad,  
Lahore Campus- Pakistan

Fall 2024



**COMSATS University Islamabad, Lahore Campus**

**Synthesis of 3D Flexible Electrode of Hybrid  
Supercapacitor Derived from Biomass via In-Situ  
Polymerization of Polyaniline a Conducting Polymer**

A Thesis Presented to

**COMSATS University Islamabad, Lahore Campus**

In partial fulfillment

of the requirement for the degree of

**MS (Physics)**

By

**Saman Anwar**

**CIIT/SP22-RPH-005/LHR**

**Fall 2024**

# Synthesis of 3D Flexible Electrode of Hybrid Supercapacitor Derived from Biomass via In-Situ Polymerization of Polyaniline a Conducting Polymer

A Post Graduate Thesis submitted to the Department of Physics as partial fulfillment of the requirement for the award of Degree of MS (Physics)

Name	Registration Number
Saman Anwar	CIIT/SP22-RPH-005/LHR

## **Supervisor**

Dr. Siddique Akhtar Ehsan

Assistant Professor, Department of Physics

Lahore Campus.

COMSATS University Islamabad, Lahore Campus.

January 2024

# Final Approval

---

This thesis titled

## Synthesis of 3D Flexible Electrode of Hybrid Supercapacitor Derived from Biomass via In-Situ Polymerization of Polyaniline a Conducting Polymer

By

*Saman Anwar*  
*CIIT/SP22-RPH-005/LHR*  
Has been approved

For the COMSATS University Islamabad, Lahore Campus

External Examiner: \_\_\_\_\_

Dr. Malika Rani  
Associate Professor/Chair Person, Department of Physics,  
The Women University Multan

Supervisor: \_\_\_\_\_

Dr. Siddique Akhtar Ehsan  
Assistant Professor, Department of Physics, CUI, Lahore

Co-Supervisor: \_\_\_\_\_

Dr. Muhammad Imran Rafiq  
Assistant Professor, Department of Chemical Engineering, CUI, Lahore

HOD: \_\_\_\_\_

Dr. Muhammad Rizwan Raza  
HOD (Department of Physics) CUI, Lahore

## Declaration

I, Saman Anwar, **CIIT/SP22-RPH-005/LHR** hereby declare that I have produced this work, which is presented in this thesis, during the scheduled period of study. I also declare that I have not taken any material from any source except referred to wherever due. If a violation of HEC rules on research project has occurred in this thesis, I shall be liable to punishable action under the plagiarism rules of the HEC.

Date: \_\_\_\_\_

Signature of the student:

\_\_\_\_\_  
Saman Anwar  
CIIT/SP22-RPH-005/LHR

## Certificate

It is certified that Saman Anwar, CIIT/SP22-RPH-005/LHR has carried out all the research work related to this thesis under my supervision at the Department of Physics, COMSATS University Islamabad , Lahore Campus and the work fulfills the requirement for award of MS degree.

Date: \_\_\_\_\_

Supervisor:

\_\_\_\_\_

Dr. Siddique Akhtar Ehsan  
Assistant Professor  
Department of Physics  
CUI, Lahore.

Head of Department:

\_\_\_\_\_

Dr. Muhammad Rizwan Raza  
Department of Physics  
CUI, Lahore.

## **DEDICATION**

This work is dedicated to my beloved family, and teachers whose encouragement and support was always there along my side to accomplish my goals.

'My Lord! Bestow on them Your mercy, as they did bring me up when I was small'.

(Quran 17:24)

## **ACKNOWLEDGEMENTS**

All the praises to Almighty Allah, who is kind and Merciful. He is the Honor of the Universe. Nothing is possible without His Mercy. From my deep heart and soul, the countless and unlimited thank to Almighty Allah, who make me able to perform this work. I also offer my humblest Dood-o-Salam to Holy Prophet Hazarat Muhammad (PBUH), Who led the universe as a torch of guidance and knowledge and Whose life is an ideal example for human being. I would like to extend my special recognition and appreciation to Dr. Siddique Akhtar Ehsan and Dr. Muhammad Imran Rafiq for being a true mentors and tremendous guides. His command of the area and his appreciative attitude will always be a memory. His advice on research have been priceless and helped me to grow in my area.

A special credit to my parents and siblings for all the hard work and sacrifices they have made for me to incent me to strive towards my dreams. I thank my mother for her prayers which were always there for me to sustain the hard times. I also pay my gratitude to my father who supported me with my every dream. Special thanks to my brother Waqas Ahmad for his wise advice, kindness, motivation and endless support in difficult times and, at the end I would also like to thank to my friend Gulnaz Amin for their kind guidance, and valuable time.

Finally, yet importantly, I am very grateful to my family for showing moral support to me throughout this time.

**Saman Anwar**

**CIIT/SP22-RPH-005/LHR**



## ABSTRACT

Next generation electronics need to be high performance, multifunctional, and environmentally friendly. Here, balsa wood slice was used as a green substrate to the flexible and rechargeable energy storage devices with excellent performance is highly desired due to the demands of portable and wearable devices. This nature derived balsa wood by partial or full removal of lignin without altering or disturbing the hierarchically aligned cellulosic structure is known as delignified wood (DW). We have synthesized a ternary composite electrode comprising balsa wood, graphene oxide, and polyaniline. The properties of the synthesized material were characterized using scanning electron microscopy (SEM), X-ray diffraction (XRD), Fourier transform infrared spectroscopy (FTIR), and Raman spectroscopy. Electrochemical testing revealed that BW/GO/PANI as electrode materials contributes to high areal specific capacitance of  $343 \text{ mF/cm}^2$  at the current density of  $0.5 \text{ mA/cm}^2$ . Utilizing this BW/GO/PANI as electrodes in a symmetric configuration supercapacitor can result in an outstanding energy density as high as  $617 \text{ m Wh/cm}^2$  at a power density of  $7172 \text{ mW/cm}^2$ . Therefore, this study provides a promising and efficient way for the preparation of ideal electrode materials for high-performance flexible energy storage devices.

## TABLE OF CONTENTS

LIST OF TABLES.....	xi
LIST OF FIGURES.....	xii
LIST OF ABBREVIATIONS.....	xiv
1 INTRODUCTION.....	1
1.1 Background.....	2
1.2 Energy Storage Devices.....	4
1.3 Capacitors.....	7
1.4 Supercapacitors.....	9
1.4.1 Construction of Supercapacitor.....	9
1.4.2 Principle of Supercapacitor.....	10
1.4.3 Types of Supercapacitors.....	11
1.5 Electric double-layer Capacitors.....	12
1.6 Pseudocapacitors.....	13
1.7 Hybrid Supercapacitors.....	13
1.7.1 Asymmetric Hybrid Supercapacitors.....	14
1.7.2 Composite Hybrid Supercapacitors.....	14
1.7.3 Battery-type Hybrid Supercapacitors.....	15
1.8 Materials for Supercapacitors.....	15
1.8.1 Carbonaceous materials (graphene oxide).....	16
1.8.2 Conducting Polymers (CPs).....	17
1.8.3 Metal oxide based Supercapacitors.....	19
1.9 Flexible electrode derived from biomass.....	19
1.10 Motivation and scope of the study.....	21
1.11 Structure of thesis.....	21
1.12 Proposed methodology.....	21
1.13 Statement of the problem.....	22
2 LITERATURE SURVEY.....	24
2.1 Literature survey of Supercapacitor.....	25

2.2	Literature of flexible electrode for Hybrid Supercapacitors.....	25
3	Experimental and Characterizations.....	31
3.1	Materials.....	32
3.2	Synthesis of Graphene Oxide (GO).....	32
3.3	Delignification of Balsa wood.....	33
3.4	Synthesis of flexible electrode of Balsa wood/GO/PANI.....	34
3.5	Characterizations.....	35
3.6	Electrochemical Performance.....	36
4	RESULTS AND DISCUSSIONS.....	38
4.1	Characterizations.....	39
4.1.1	Scanning electron microscopy.....	39
4.1.2	Fourier transform infrared spectroscopy of graghite, GO, and rGO.....	40
4.1.3	Fourier transform infrared spectroscopy of BW/GO/PANI flexible electrode.....	42
4.1.4	Raman spectroscopy.....	42
4.2	Electrochemical Performance.....	43
5	CONCLUSION.....	48
6	REFERENCES.....	49

## LIST OF TABLES

Table 1.1 Comparison of various materials according to their specific parameter for supercapacitor applications.....	18
--	----

## LIST OF FIGURES

Fig 1.1 Ragone plot for different energy storage systems.....	3
Fig 1.2 Classification of supercapacitors based on cyclic voltammetry .....	4
Fig 1.3 Electrochemical Energy Storage Devices.....	5
Fig 1.4 Schematic of a secondary battery during (a) charging and (b) discharging.....	6
Fig 1.5 The Parallel -Plate Capacitor.....	7
Fig 1.6 Charge Inside the Capacitor.....	7
Fig 1.7 Development History of Advance Capacitor.....	8
Fig 1.8 Schematic illustration of Principle of Supercapacitor.....	10
Fig 1.9 Schematic illustration of the charging and discharging phenomena.....	11
Fig 1.10 Types of Supercapacitors.....	11
Fig 1.11 Electric Double-Layer Capacitor (EDLCs).....	12
Fig 1.12 Schematic Illustration of Pseudocapacitor (PCs).....	13
Fig 1.13 hybrid Supercapacitors.....	14
Fig 1.14 Structure of Graphene, Graphite, GO and rGO.....	17
Fig 1.15 Transforming wood as next generation.....	19
Fig 3.1 Synthesis of Graphene Oxide (GO).....	31
Fig 3.2 Delignification of Balsa wood.....	32
Fig 3.3 Practical demonstration of mechanical strength and flexibility for FBW.....	32
Fig 3.4 Synthesis of flexible electrode of balsa wood/GO/PANI.....	33
Fig 3.5 Flexibility of balsa wood after polymerization is retained.....	33
Fig 3.6 Technique for characterizing materials that is suggested to investigate their chemical and physical characteristics.....	34
Fig 3.7 suggested plan to examine the material used in supercapacitors to investigate Its electrochemical performance.....	35
Fig 4.1 SEM images of delignified balsa wood.....	38
Fig 4.2 FTIR spectrum of a) Graphite powder b) Graphene oxide c) Reduce Graphene Oxide.....	39
Fig 4.3 FTIR spectrum of Pristine balsa wood, Delignified balsa wood, and Synthesized BW/GO/PANI composite.....	40

Fig 4.4 Raman spectroscopy of BW/GO/PANI.....	41
Fig 4.5 CV curves of BW/GO/PANI at different scan rates.....	43
Fig 4.6 GCD curves of BW/GO/PANI at different current densities.....	44
Fig 4.7 EIS performance of BW/GO/PANI flexible electrode.....	45

## LIST OF ABBREVIATIONS

EES	Electrochemical Energy Storage
EDLCs	Electric double-layer capacitors
UV	Ultra violet
SCs	Supercapacitors
MOF	Metal organic framework
GO	Graphene Oxide
rGO	Reduce graphene oxide
CNTs	Carbon Nanotubes
MWCNTs	Multiwalled carbon nanotubes
CPs	Conducting Polymers
PANI	Polyaniline
PPy	Polypyrrole
PEDOT	Poly (3,4-ethylenedioxythiophene)
PSS	Poly (styrene sulfonate)
PTH	Polythiophene
AC	Activated carbon
FBW	Flexible balsa wood
PDW	Partially delignified wood
LBL	Layer by layer
MMM	Mixed matrix membrane

**Chapter 1**  
**Introduction**



## 1.1. Background

Fossil fuels, such as coal, oil, and gas, which make up the majority of the world's energy supply and are responsible for more than 75% of all greenhouse gas emissions and almost 90% of all carbon dioxide emissions, are by far the biggest contributors to climate change[1]. Emissions must be cut in half by 2030 and net-zero by 2025 in order to prevent the worst effects of climate change. To do this, we must stop relying on fossil fuels and instead invest in clean, readily available, cost-effective, sustainable, and dependable alternative energy sources. To promote sustainable development, it is crucial to use energy effectively and generate clean, renewable energy sources [2]. The rapidly expanding markets for portable electronics and electric vehicles encourage the development of energy storage technologies with high energy and power densities that are also environmentally friendly.

So, in this scenario researchers are paying close attention to wood and its derivatives as potential electrode materials for Energy Storage System (EES) devices[3]. Wood-derived materials have garnered a lot of attention in the last ten years for both basic research and real-world applications in a variety of functional devices. Wood-derived materials are ideal for effective energy storage and conversion because they are renewable, abundant naturally, environmental friendly, and biodegradable. They also have a hierarchically porous excellent mechanical flexibility and integrity and tunable multifunctionality [4][5][6].

Over the past few decades, supercapacitors—also known as electrochemical capacitors and ultracapacitors—have been explored as energy storage devices with high power capability, great reversibility (90–95% or higher), and a long cycle life (>10<sup>5</sup> cycles) [7][8]. Based on how they function, supercapacitors may be broadly divided into two categories: There are two types of electrical double-layer capacitors (EDLCs): (1) carbon-based supercapacitors, which derive their capacitance from the charge separation at the electrode/electrolyte interface; and (2) Pseudocapacitors, which derive their capacitance from reversible faradic reactions at the electrode surface, such as transition metal oxide-based supercapacitors.

Supercapacitors are becoming increasingly popular for their extended cycle efficiency, quick charging-discharging stability, and high-power density but the energy density of supercapacitor is very low as compared to batteries[9]. Due to the high capacity and large potential window rechargeable batteries exhibits high energy density but their power density is very low. Therefore,

no single tool can satisfy the needs of the market alone. Hybrid energy storage technologies, which combine the benefits of supercapacitor and rechargeable batteries, have been created and developed as a solution to this problem.

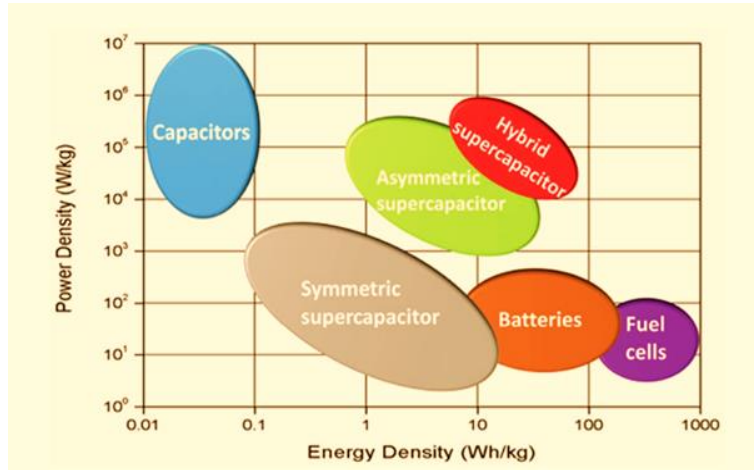


**Fig. 1.1** Ragone plot for different energy storage systems.

Figure 1.1 The specific energy and specific power of common energy storage and conversion devices are displayed in the Ragone plot [7].

Hybrid supercapacitor is physically a combination of a supercapacitor with the chemistry of a battery. In order to overcome the distinct drawbacks of batteries and supercapacitors, hybrid supercapacitors combine the physics of a supercapacitor with the chemistry of a battery in a single structure. Hybrid supercapacitors store charge using both faradic and non-faradaic reactions both powered density and energy density are maintained simultaneously by them, however neither measure is larger than Pseudocapacitor and EDLC specifications. Their cyclic voltammetry curve, as mentioned, has a minor hump that is visible and deviates somewhat from the rectangular form of ordinary EDLCs.

As a consequence, these hybrid devices provide definite advantages. As we've shown, EDLCs provide good cycle stability and power performance, and in the case of pseudo capacitance, they provide a higher specific capacitance. By combining a power source that is similar to a capacitor electrode and an energy source that is similar to a battery electrode in the same cell, a hybrid system provides a mix of both. Increased cell voltage, which in turn improves energy and power densities, is achievable with the right electrode configuration. Future energy storage systems for

wearable, implantable, and portable electronics can greatly benefit from the use of hybrid supercapacitors.

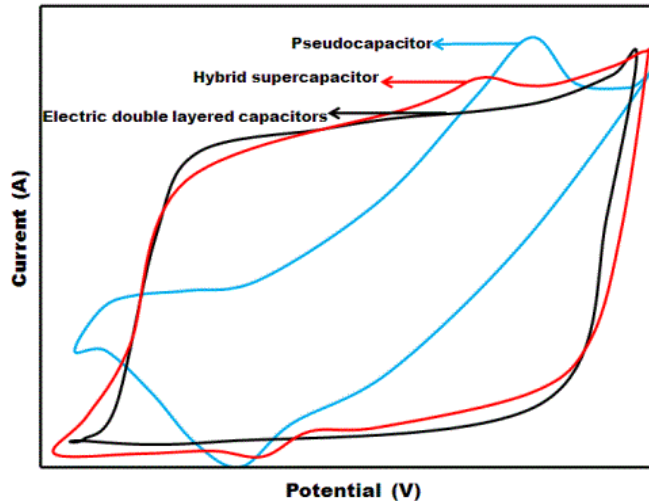


Fig 1.2 Cyclic voltammetry-based supercapacitor categorization[8].

## 1.2 Energy Storage Devices

Our existing way of life cannot be sustained without electrical energy. The depletion of natural fossil fuel supplies occurs every ten years, making the switch to electric-powered vehicles and household energy usage imperative for maintaining our level of life in the future. Furthermore, because of the emission of greenhouse gases, the overuse of fossil fuels in recent decades has resulted in catastrophic climatic changes. The production, storage, and use of renewable energy sources can help to lessen these negative consequences.

Energy storage devices are necessary because, when power is produced, it has to be effectively stored for use in portable applications, electric cars, and other times when demand is high [10]. The ability to capture, store, and release electrical or chemical energy as needed is made possible by energy storage devices, which are essential parts of contemporary energy systems. In order to effectively integrate renewable energy into the grid, these devices are essential in overcoming the problems caused by intermittent renewable energy sources like solar and wind. Batteries, including lithium-ion and solid-state versions, store electrical energy for a variety of uses, including grid-scale energy storage, electric cars, and portable gadgets. On the other side, fuel cells make it possible to convert chemical energy, frequently hydrogen, into electricity while minimizing pollutants, making them a viable option for both stationary and mobile power generation.

Additionally, energy storage technologies using pumped hydro, flywheels, and compressed air provide distinctive options for grid-scale energy.

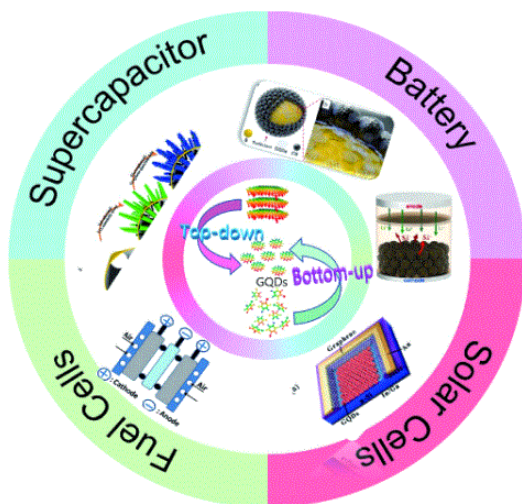


**Fig 1.3** Electrochemical Energy Storage Devices

There are several known electrochemical energy storage systems, including fuel cells, batteries, solar cells and supercapacitors. Hydrogen is commonly used as a fuel source for fuel cells, however it is a secondary source of energy and does not occur naturally. The viability of fuel cell automobiles and stationary applications is constrained by the absence of a significant hydrogen infrastructure.

In order to convert sunlight into electricity, solar cells, sometimes referred to as photovoltaic cells, are essential parts of renewable energy systems. They provide several advantages, including minimal running costs and environmental sustainability. However, a number of problems, including intermittency, energy storage, initial outlay, space requirements, and aesthetics, among others, have prevented their widespread use. The photovoltaic effect is the basis for how solar cells work. The mechanism by which some materials produce an electrical current when exposed to light is known as the photoelectric effect. Two major hurdles in this technology are quantum efficiency and the durability of solar cell devices under prolonged exposure to high UV radiation. These solar cells may gradually deteriorate from exposure to harsh climatic factors, such as the intense heat of deserts and the bitter cold of the poles, which would eventually reduce their quantum efficiency.

The most prevalent and well-known kind of energy storage are batteries. Energy storage applications frequently employ secondary batteries, also known as rechargeable batteries[11]. Rechargeable batteries are frequently used as an energy source in consumer gadgets like computers and cell phones. When charging and discharging secondary batteries, also known as rechargeable batteries, reversible electrode reactions occur.

Batteries have a shorter lifespan than supercapacitors because these redox reactions are not totally reversible. Additionally, supercapacitors' quick electrostatic charge separation outperforms batteries' sluggish chemical processes, resulting in prolonged charge and discharge periods.

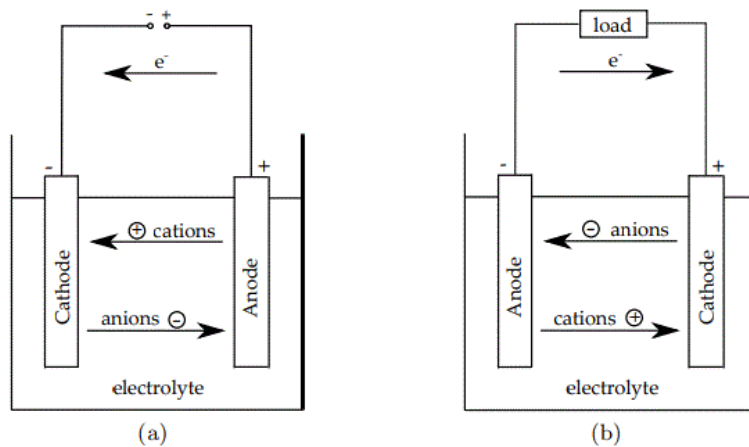


**Fig 1.4** Schematic of a secondary battery during (a) charging and (b) discharging (adapted from [11]).

In addition, there are few risks connected to the use of batteries, such as the release of harmful substances like mercury, lead, or cadmium metals as their electrode or electrolyte, or the ingestion of batteries[12].

### 1.3 Capacitors

Energy storage technologies at the outset of electrotechnology could be divided into three categories: (1) Inductors, which stored energy using a magnetostatic field; (2) Batteries, which stored energy through chemical reactions; and (3) Capacitors, which stored energy using an electrostatic field. An essential component of electrical circuits, a capacitor has two electrical terminals and functions as a passive electrostatic energy storage device.

Capacitors come in a variety of forms, but they all consist of two electric conductor plates that are spaced apart by a dielectric substance.

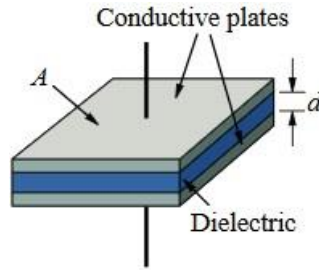


Fig 1.5 The Parallel -Plate Capacitor

Consider merely the parallel plate capacitor, as shown in Figure 2.3, where a uniformly thick dielectric material separates the two conductors or electrodes. Any substance that readily conducts electricity can be used as a conductor. The dielectric needs to be an insulator and a poor conductor. The charge capacity of capacitors is increased by a non-conductive dielectric. An electric field is created when charges attempt to accumulate on two electrodes in response to an external voltage application. Its ability to store electrical energy is due to the electric field.

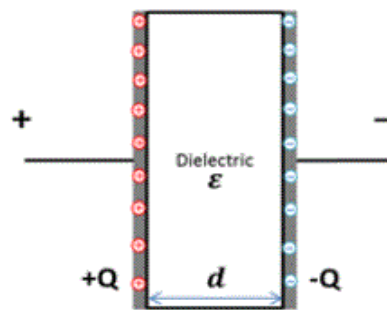


Fig 1.6 Charge Inside the Capacitor

Capacitors can be made of many different materials, such as discs, aluminium foil, or thin layers of metal. The Leyden jar's creation in 1745 marked the beginning of capacitor technology[13]. After that, one after another a row of representative capacitors emerged. Paper capacitors were first created in 1876 by tightly wrapping a waxed piece of paper between two metal foils to form a circular column[14]. Using alumina as the dielectric and a less impurity etching aluminium leaf, the first electrolytic capacitor was invented in 1896[15]. The mica dielectric capacitor (1909), the polyethylene terephthalate-based capacitor (1941), and the plastic dielectric capacitor (1959) are a few notable capacitors that have also emerged one after the other[16].

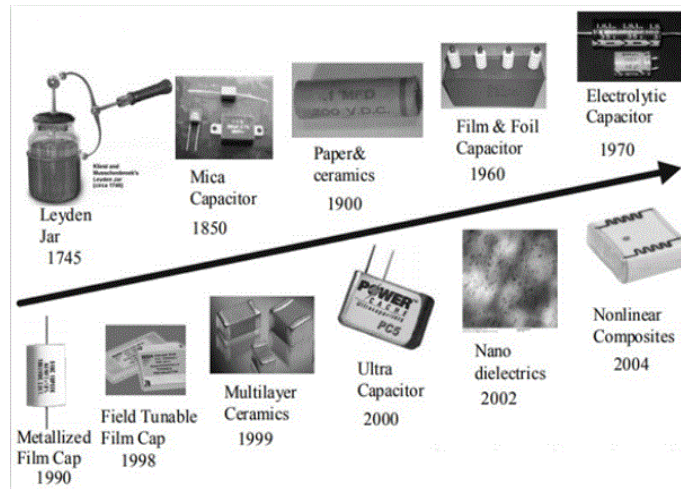


Fig 1.7 Development History of Advance Capacitor

An essential feature of a capacitor is its capacitance, which establishes the relationship between electrical charge and voltage:

$$C = \frac{Q}{V} \quad (2.1)$$

The capacitance will change when the voltage changes. In this case, the capacitance expressed as follows:

$$C = \frac{dQ}{dV} \quad (2.2).$$

The voltage in a capacitor consisting of two parallel plates separated in surface area by a permittivity-distributed dielectric and thickness is recognized as the crucial element of the electric field concerning the separation. Thus, the capacitance may be shown as follows:

$$C = \frac{\epsilon A}{d} \quad (2.3)$$

The following represents the energy stored in a capacitor:

$$E = \frac{1}{2} CV^2 = \frac{Q^2}{2C} \quad (2.4)$$

The discharge time of a capacitor is required to determine its power density.

$$P = \frac{E}{\Delta t} \quad (2.5)$$

The need for less intense, and bulky capacitors with extended temperature capabilities is rising in the military, drilling for oil and gas, power electronics, and hybrid car industries. Growing temperature rating is one of the most intricate technological obstacles in energy density that has

been found. Better insulation and capacitor development would allow the operating system to function at temperatures between 150-300 °C, which would be necessary to create the small, light systems of the future.

## **1.4 Supercapacitor**

One form of novel energy-saving technology that converts energy is the supercapacitor. Supercapacitors, or SCs, are significant because of their unique characteristics, which include long cycle life, high strength, charge/discharge period, specific capacitance and environmental friendliness[17]. They also share fundamental equations with traditional capacitors; to achieve high capacitance, SCs use electrode materials with thinner dielectrics and high specific surface area.

Many porous materials are commonly used in the construction of supercapacitors, including metal organic frameworks, many carbon-based MOF composites, and numerous additional composites (such as carbon-based NiO and FeO composites) because of their extensive electrochemical capabilities[18]-

The performance of the composites was evaluated using metrics such as energy, cycle performance power, capacitance, and rate capability, which also provides information on the electrolyte materials.

### **1.4.1 Construction of Supercapacitor**

Supercapacitors are typically made up of three main parts: packaging, electrolyte, separator, and active material, which consists of electrodes. The materials that are active are used as electrodes. A three-electrode system consists of working, counter, and reference electrodes. Standard materials, such as Ag/AgCl or Hg/HgCl, are used to create the reference electrode, and platinum or graphite wire, which has a high corrosion resistance, is used to create the counter electrode. The working electrode is assumed to be the material under inquiry.

### **1.4.2 Principle of supercapacitor**

The capacitors store energy by using electrostatics, or static electricity. The electrolyte fluid between the two plates of the supercapacitor contains both positively and negatively charged ions. When a voltage is applied across one of the supercapacitor's plates, a positive charge usually



accumulates, while a negative charge often develops on the other plate. Consequently, the electrolyte solution's negative ions are pulled to the positively charged plate and the positively charged ions are drawn to the negative metal plate. A small layer of ions is deposited on the inner surface of both plates. This results in an electrostatic double layer, which is comparable to connecting two capacitors in series. The basic principle behind supercapacitor energy storage is the electric double-layer capacitance produced by charge separation at the interface between the electrolyte and the bath solution. Because supercapacitors have a larger surface area and fewer spaces between electrodes, their capacitance and energy rise dramatically.

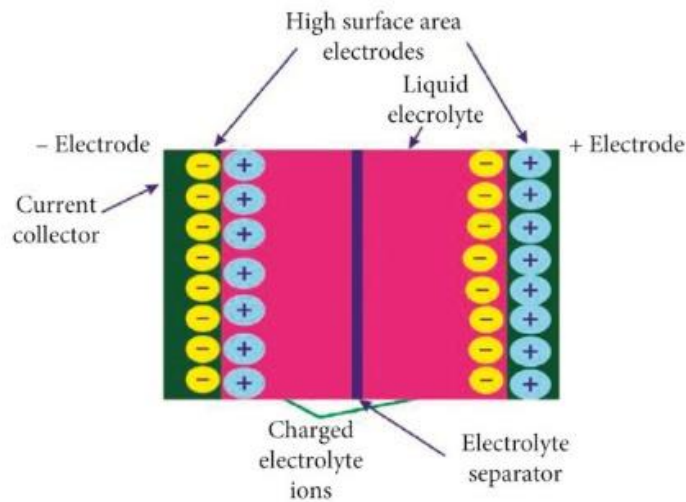


**Fig 1.8** Schematic illustration of Principle of Supercapacitor

On the negative and positive electrode surfaces, respectively, positive and negative (electrons) charges are stored during charging. The process is reversed during the discharge period, as observed in the intermediate state, and the ions seem to be moving randomly. Ultimately, the charged ions fall to the surface of the electrodes across from one another after being released from the electrodes. A cycle is finished in this manner. For more cycles, the supercapacitors are then charged once again. In comparison to batteries, supercapacitors show suitable discharge times and are charged more quickly. Because they retain the best possible power and energy densities, supercapacitors are preferable over batteries.

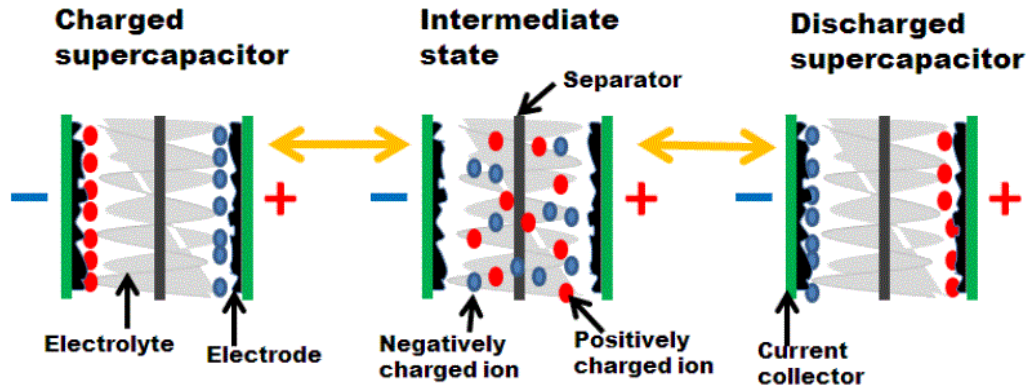


Fig 1.9 Schematic illustration of the charging and discharging phenomena

### 1.4.3 Types of Supercapacitors

Supercapacitors may be categorized into three primary groups according to their functioning mechanisms:

1. Electrostatic double-layer capacitors
2. Pseudo-capacitors
3. Hybrid capacitors

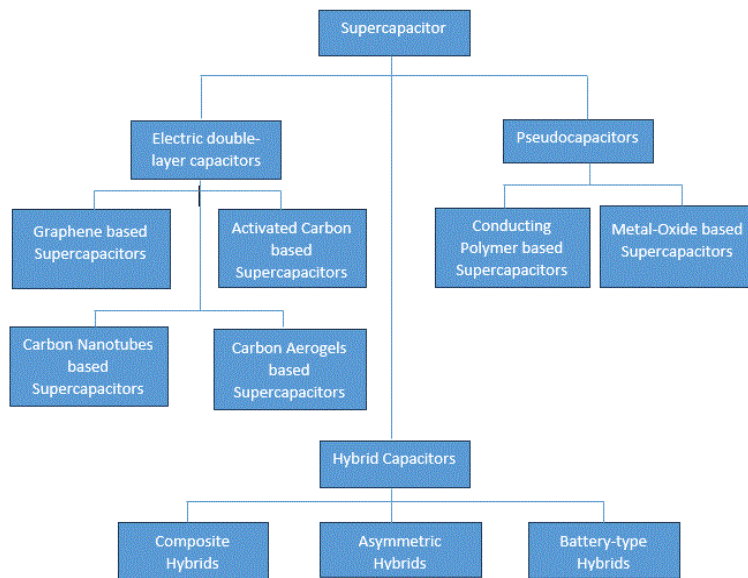


Fig 1.10 Types of Supercapacitors

## 1.5 Electric double-layer Capacitors

The electric double-layer capacitor (EDLC), commonly referred to as a supercapacitor, stores energy via the electrostatic charge separation technique. When a voltage is supplied, it functions without causing a chemical reaction and builds up charges on the electrode surfaces. As electrolyte ions pass through a separator and into electrode pores, the applied voltage causes opposing charges to accumulate at the electrode-electrolyte interface.

A stable double layer is formed and maintained by carefully controlling the electrode engineering process to prevent ion recombination. Due to its ability to store and discharge energy quickly and effectively, EDLCs are a good fit for applications like electronic devices and transportation that need for high power density and quick energy transmission.

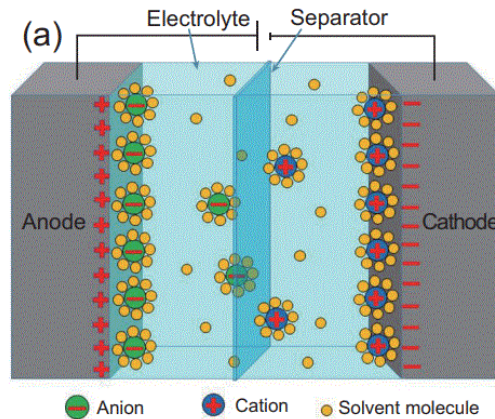


Fig 1.10 Electric Double-Layer Capacitor (EDLCs)

## 1.6 Pseudocapacitors

Pseudocapacitors function with oxidations and reduction peaks at the electrode surface and store energy via reversible redox processes or Faradaic reactions. When compared to electric double-layer capacitors (EDLCs), faradaic reactions improve specific capacitance and energy density by enabling charge storage electrostatically. On the electrode material, voltage application causes simultaneous reduction and oxidation. Metal oxides and conducting polymers are the two main types of electrode materials used in pseudocapacitors, which effectively store charges in these energy-storage devices[13]. Pseudocapacitors are suited for rapid charge and discharge applications such as regenerative braking in vehicles because they have a higher power density

and longer lifespan. Because of their high capacitance and low cost, pseudocapacitive materials are used in supercapacitors, which maximizes the affordability and efficiency of energy storage applications[19]. They cannot, however, be used for long-term energy storage due to their reduced energy density and nonlinear charge-to-voltage output voltage drop.

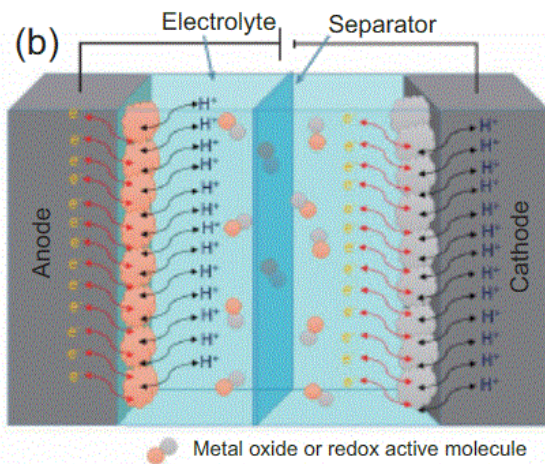
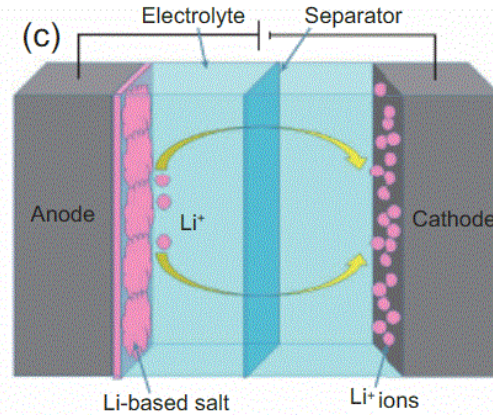


Fig 1.11 Schematic Illustration of Pseudocapacitor (PCs)

## 1.7 Hybrid Supercapacitors

Battery chemistry and supercapacitor physics are combined in hybrid supercapacitors, which combine the architectures of the two components into one single device. Compared to Li-ion batteries, these asymmetric devices combine electrochemical charge movement at a shallower depth with a Li-doped graphite anode and an activated carbon cathode. Outstanding results from this technology include a cycle-life count of at least 500,000 cycles and quick response to high discharge rates. Furthermore, since no metal oxides are utilized, there is no chance of thermal runaway or fire with these hybrid supercapacitors. Recent advances in energy storage technology have led to the popularity of hybrid supercapacitors, which offer higher energy densities without sacrificing power density[20].



**Fig 1.12** Hybrid Supercapacitor

### 1.7.1 Asymmetric Hybrid Supercapacitors

Hybrid supercapacitors exhibit asymmetric behavior that increases their capacitance values by combining the features of a pseudocapacitor and an electric double-layer capacitor (EDLC). This creative strategy is a positive step towards long-lasting, effective, and pollution-free energy storage options. For instance, Rodrigo Henriquez and associates [21] created a novel hybrid supercapacitor in 2021 by employing AC as the negative electrode and a combination of CdCO<sub>3</sub>/CdO/Co<sub>3</sub>O<sub>4</sub> as the positive electrode. This hybrid supercapacitor used both faradaic and non-faradaic techniques to store energy, resulting in good specific power and much greater specific energy. In comparison to Electric Double-Layer Capacitors (EDLCs), asymmetric hybrid supercapacitors may reach higher energy and power densities and have superior cycle stability.

### 1.7.2 Composite Hybrid Supercapacitors

Integrated carbon materials with metal oxides or conducting polymers as electrode materials set composite hybrid supercapacitors apart from asymmetric hybrids. Through faradaic processes, conducting polymers or metal oxides increase capacitance, while porous carbon increases surface area and improves interaction with the electrolyte. In supercapacitor applications, conducting polymers and carbon-based materials are essential since they are capacitive materials. However, their low capacitance, limited lifespan, and poor rate capabilities limit their employment as independent devices[22].

### **1.7.2 Battery-Type Hybrid Supercapacitors**

Battery-type hybrids, which have both a battery electrode and a supercapacitor electrode, are a promising class of energy storage systems. Battery-type hybrids have the potential to be very important because, with proper design, they can combine the high energy density of batteries with the specific power, fast charge times, extended cycle life, and reversibility of supercapacitors. Essentially, the combination of these two technologies into a single hybrid system means that the drawbacks of separate energy storage devices can be addressed because the system's versatility could be enhanced by combining the best features of batteries and supercapacitors.

### **1.8 Materials for Supercapacitors**

Wood's weak conductivity restricts its uses. Because of their better conductivity, chemical and thermal stability, and affordability, carbon-based electrode materials such as graphene, carbon nanotubes, and activated carbon are preferred[23]Owing to their beneficial properties, porous carbon materials are the preferred option for supercapacitor electrodes. The pursuit of large capacitances highlights the inclination towards highly conductive carbons with large surface areas. The most researched and promising electrode materials for a variety of applications are carbon-based materials such as graphene, Mexene, carbon nanotubes (CNTs), porous carbon, and conducting polymers like polypyrrole (PPy), polyaniline (PANI), and poly(3,4-ethylenedioxythiophene): poly(styrene sulfonate) (PEDOT:PSS[24][25]. The incorporation of pseudocapacitive materials has arisen as a way to boost capacitance levels, despite the comparatively low specific capacitance of carbon-based materials. Pseudocapacitive materials are coated onto the carbon infrastructure in this way to provide flexible electrodes with increased specific capacitance. In particular, current research has concentrated on coating different polymer compounds or metal oxides on carbon substrates to create carbon composite materials. offering a dynamic method for enhancing the performance of the supercapacitor electrode.

Conducting polymers and metal oxide exhibit excellent pseudocapacitance. The use of conducting polymers and metal oxides in supercapacitor technology is limited because they are less cyclically stable during charging and discharging. Because of their high conductivity, reversible faradaic characteristics, low cost, and high energy density, conducting polymers have been employed widely in supercapacitor devices. Products including PANI, Ppy, and polythiophene have also been investigated for use as supercapacitor electrode materials[26].

In order to address this issue and satisfy the need for energy storage, composites are being employed as electrode materials, which may enhance supercapacitor performance.

### **1.8.1 Carbonaceous Materials (graphene oxide)**

There are many different types of carbon in the world, but one of the most well-known is found in minerals and is called graphite. A semimetal called graphite has a crystalline structure made up of many bulk planar layers of carbon atoms. Graphite oxide is the substance that results when different proportions of hydrogen and oxygen are incorporated into these carbon layers. Graphite oxide usually takes on an irregular form with high particle sizes, in contrast to the regular structure of graphite. Though graphite is the parent allotrope, graphite oxide has unique physical characteristics that distinguish it from graphite.

Additionally, another allotrope of carbon is graphene oxide (GO). Numerous techniques developed by Staudenmaier, Hofmann, Brodie, Hummers, and others can be used to synthesize GO. In 1859, Brodie created the first GO synthetic. The most famous is the Hummers method, which he published in 1958. A modified Hummers' technique was used to oxidize the graphene in order to produce graphene oxide[27].

The GO dissolves more easily in ethanol, water, N-N dimethylformamide, and a few other organic solvents, however it may be loosely mixed with any solvent. Graphene oxide (GO) has a high specific surface area and charge carrier mobility, making it a promising material for use in electronics, catalysis, and energy storage[28]. Graphene oxide is thought to be a superior option than graphene for the electrode material in supercapacitors due to its excellent performance and affordable price[29]. Reduced graphene oxide nanosheets (rGO NSs) and graphene are examples of a novel family of two-dimensional carbon nanostructures. In recent years, its distinct attributes like as chemical stability, large surface area, and broad electrochemical window have rendered it a highly appealing option for supercapacitor electrode material [30]. With its remarkable performance in terms of high energy storage, high power density, and extended cycle life, graphene/rGO-metal oxide-based hybrids and composites have found broad application in electrochemical capacitors[31]. Specifically, the manufacture of rGO on a wide scale at a reasonable cost from graphite powder using chemical oxidation/reduction techniques has attracted international interest and established its demand as an electrode material for supercapacitors.

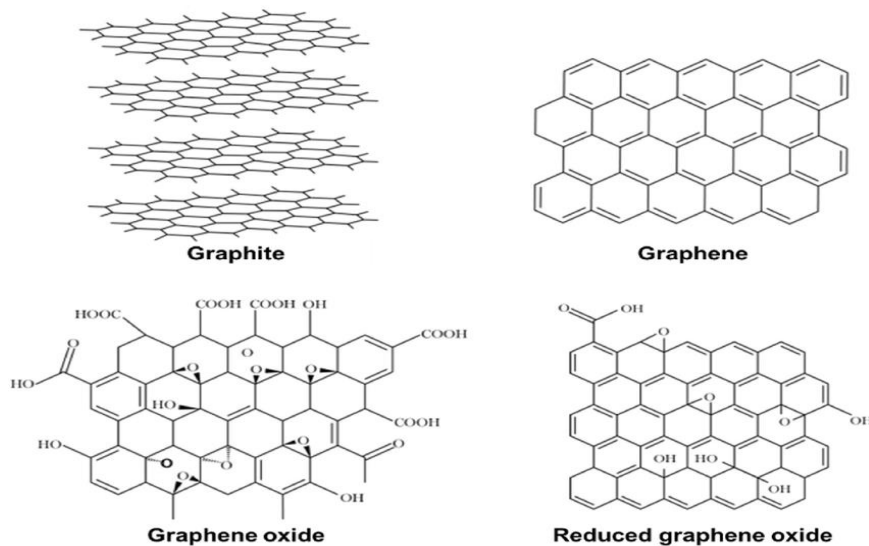


**Fig 1.13** Structure of Graphene, Graphite, GO and rGO

## 1.8.2 Conducting Polymers (CPs)

Cutting edge electronic applications might be greatly enhanced by modern materials like flexible supercapacitors. Conducting polymers (CPs) are among the most promising pseudocapacitor materials for the construction of flexible supercapacitors, pushing the current generation of energy storage devices towards the next generation of advanced flexible electronic applications due to their high redox active-specific capacitance and intrinsic elastic polymeric nature [32].

In the recent development of CPs-based flexible ES applications, many approaches have been employed to use either CPs alone or composites of CPs with carbon materials as the electrode materials.



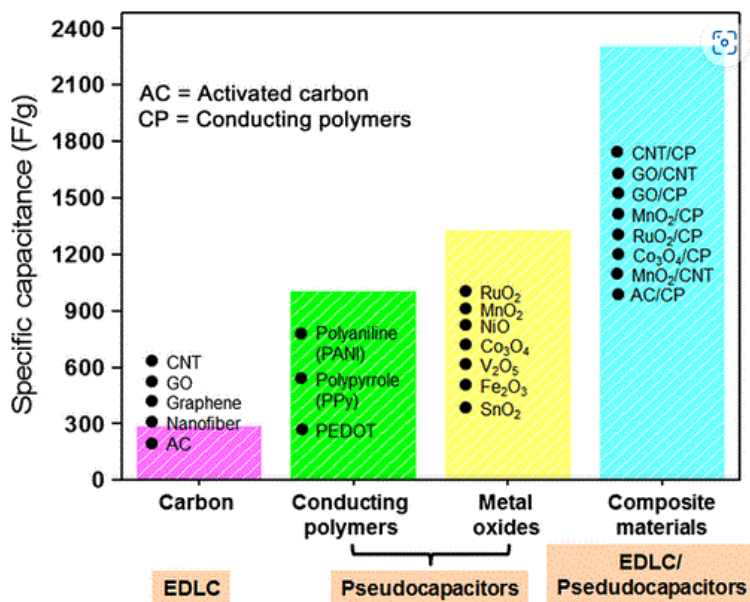


**Table 1.** Comparison of various materials according to their specific parameter for supercapacitor applications[32].

In addition to being investigated for their potential to increase conductivity and cycle life, composite electrodes may also have other physical characteristics based on the interactions between the various parts. Because carbon-based binary composites are more readily available in different forms and have higher mechanical strength, conductivity, and stability than other oxide-based composites, they have received more attention in the recent development of flexible CPs-based supercapacitors.

Principally, polyaniline (PANI), polythiophene (PTH), polypyrrole (PPY), and their byproducts are conjugated conducting polymers[33][34]. One polymer that is very conductive is PANI. Owing to its distinct characteristics, ease of synthesis, affordability, and superior stability in many applications including pharmaceuticals, electronics, and anti-corrosion materials, it has garnered significant interest[35].

### 1.8.3 Metal Oxides based Supercapacitors

Hybrid supercapacitors based on metal oxides combine additional materials with the beneficial features of metal oxides to improve energy storage efficiency. These hybrids frequently combine carbon-based materials, conducting polymers, or other nanomaterials with metal oxides such as

ruthenium oxide (RuO<sub>2</sub>) or manganese dioxide (MnO<sub>2</sub>). These combinations work in concert to increase overall electrochemical performance, cycle stability, and capacitance. Because of their adaptability, metal oxide-based hybrid supercapacitors have great promise for applications that need high energy density and effective cycles of charge and discharge. This will help to develop the fields of electric cars and portable electronics.

Bimetallic oxide materials are far more attractive than single metal oxides because they can produce a high capacitance, boost the energy density at this capacitor-level power, and get around the problem of single metal oxides' poor electric conductivity [36]. A new electrode made of cobalt oxide has been employed in supercapacitors. A specific capacitance of 785 F/g with 20% carbon nanotube loading and 322 F/g in a 6 mol/L KOH solution were attained[37].

### 1.9 Flexible electrode derived from Biomass

Wood-derived materials have garnered a great deal of attention in the last ten years for both practical applications in a variety of functional devices and basic research[3][38]. The wood-based materials are abundant, renewable, and environmentally friendly[4], which makes them perfect for electrochemical energy storage (EES) device components like electrodes, current collectors, separators, and template/substrate materials.

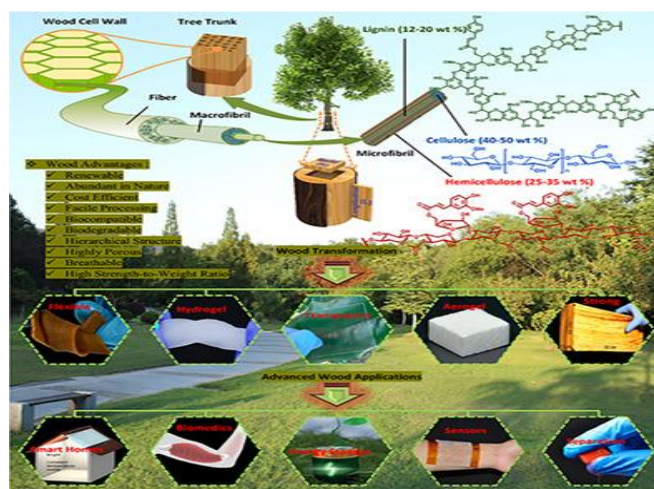


Fig 1.15 Transforming wood as next generation[39]

Wood-derived materials are ideal for efficient energy storage and conversion because they have several unique advantages, including excellent mechanical flexibility and integrity, tunable

multifunctionality, and hierarchically porous structures (such as vertical channels and numerous micro/nanopores) for fast transport of electrons and ions [5].

Non-carbonized wood has recently surfaced as a mechanically durable scaffold for cutting-edge functional electronics[40]. A large number of tube-shaped cell walls aligned in a certain way provide NW its structural integrity and are essential to wood's mechanical strength. The chemical alterations brought about by the physical alteration of cell walls demonstrate a notable rise in wood's mechanical strength.

To be more precise, the chemical alterations aid in the process of creating flexible wood (FW). Recently, delignification has been recommended again to increase the mechanical strength, porosity, and functionalizability of wood. By eliminating lignin and hemicellulose from cell walls, this mechanism expands the number of micropores and mesopores in the structure[41][42]. Wood scaffolds therefore get a lot of porosity and hydroxyl functionalities in addition to having their native structure retained. These fibre porous templates are easily modified and functionalized further. Wood-based electrodes have distinct benefits over traditional electrode materials, including the ability to produce high areal mass loading of active materials, higher mechanical performance, excellent electronic conductivity, and a hierarchically porous structure[43].

### **1.10 Motivations and scope of the study**

Because of finite resources and decades of inefficient energy consumption, we are facing a worldwide energy crisis. Effective energy storage is essential. Supercapacitors are one of the most promising solutions since they are effective energy storage devices with high specific capacitance, energy density, power density, and an impressive lifespan. Supercapacitors exhibit weather independence and environmental friendliness in addition to being more affordable and lightweight than alternative energy storage technologies. There is a noticeable trend towards the usage of carbonaceous (GO) based composites as electrode materials despite the variety of materials used in supercapacitor applications. It is anticipated that these materials will improve supercapacitor performance considerably.

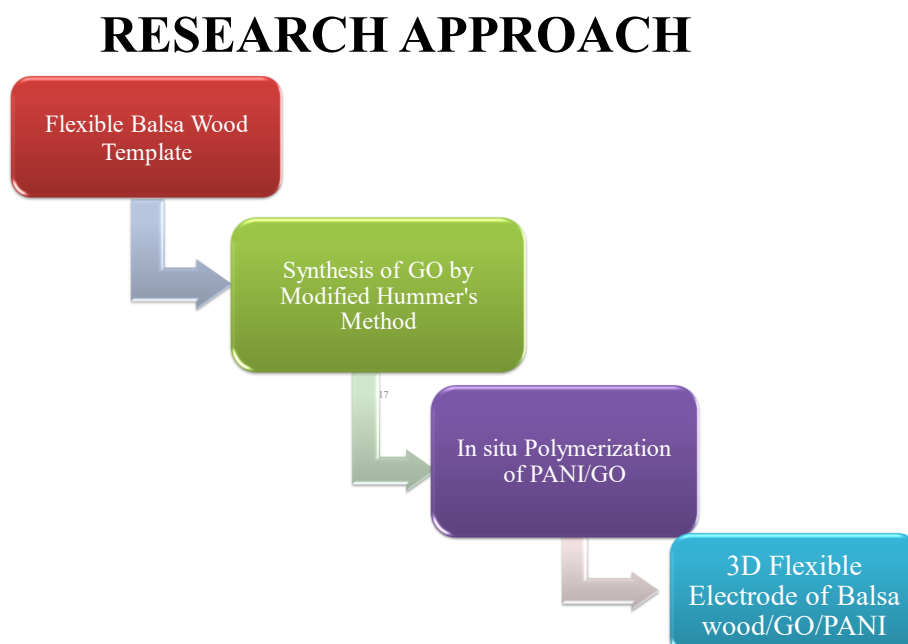
### **1.11 Structure of Thesis**

The provided material is divided into five chapters. The first chapter includes a description of the study's goals and objectives as well as an overview of energy storage technologies and carbonaceous materials including graphene oxide, reduced graphene oxide, and graphene. The

reason for the investigation and its technical significance are also included in order to illustrate the scientific merit of the current effort. A review of the literature on conducting polymers, metal oxide, carbonaceous materials, and their composites is presented in the second chapter. The experimental techniques applied to the synthesized goods' growth and inspection are described in detail in the third chapter. In chapter four, the results and debate are explained. Chapter 5 concludes with recommendations for future directions and technological applications, along with a few gaps that need to be filled in future.

## 1.12 Proposed Methodology

In this work, it is more suited to use in-situ polymerization of a suitable conducting polymer to create 3D flexible electrode of a hybrid supercapacitor that is derived from biomass.



Scanning electron microscopy (SEM) and X-ray diffraction (XRD) can be used to clarify the morphological and structural features, respectively. Fourier-transform infrared spectroscopy (FTIR) is used to determine the structures and functional groups of organic molecules. Additionally, Raman Spectroscopy is used to measure the molecular structure and chemical composition. Through electrochemical testing using galvanostatic charge and discharge,

electrochemical impedance, and cyclic voltammetry, the real electrochemical properties of the synthesized product may be determined.

### **1.13 Statement of the Problem**

Studying the charge storage mechanism and energy density of the various materials is necessary to increase the supercapacitors' electronic conductivity and efficiency. Many efforts are still being made in practice because high specific capacitance, energy density, and stability electrodes are needed. Supercapacitors use carbon-based electrode materials because they are more affordable, have improved conductivity, and are resistant to heat and chemicals. However, their specific capacitance is lower. Composites are being used as electrode materials to alleviate this problem, which might improve supercapacitor performance. Therefore, in order to get over a number of obstacles such high cost, low energy density, and short battery life, we will employ a combination of graphene oxide (GO) and polyaniline (PANI) in our study proposal.

## **Chapter 2**

### **Literature Survey**

## **Literature Survey**

The literature review of different energy storage technologies is presented in this chapter in order to make distinctions between them. Also covered is a review of the literature on the various materials that are utilized to create flexible electrodes for hybrid supercapacitors. The analysis of the materials that have been published has also been explained in detail to highlight the different materials such as oxide, carbonaceous, and polymers that are used in supercapacitors.

### **2.1 Literature Survey of supercapacitor**

Supercapacitors are said to be the most efficient energy storage technology because of its high specific capacitance, extended life, and suitable energy density and power density values [4]. Figure 1.1 displays the Ragone plot for a variety of energy storage systems, plotting power density vs energy density. Additionally, these are low maintenance, lightweight, and environmentally friendly [44]. Batteries have a comparatively higher power density than fuel cells, despite the fuel cell having a higher energy density than all other energy storage systems. It is challenging to store a large quantity of energy and then distribute it at faster rates since typical capacitors have a high-power density but a low energy density. Supercapacitors are therefore well-known and effective devices because of their very wide range of suitable energy and power density, which allows them to store large amounts of energy and subsequently deliver it at a very rapid pace [45].

### **2.2 Literature survey of flexible electrode for Hybrid Supercapacitor**

The transition of human reliance from limited fossil fuel-based resources to renewable and sustainable resources will determine the course of sustainable development in the future. High performance, ecologically friendly material design will need the use of scalable assembly techniques. This is due to the fact that new procedures that permit control at every level of hierarchy will be needed. Wood may be simply described as a biological engineering material consisting of cellulose fibrils embedded in a matrix of hemicelluloses and lignin, forming a complex hierarchical structure.

- Yi Chen, et al. reported the development of a totally wood-based flexible electronics circuit that satisfies next-generation specifications. The substrate is a robust, flexible, and translucent wood film that is coated with a conductive ink made of carbon nanofibers generated from lignin. In order to customize the material's nanostructure, lignin and hemicellulose must be extensively removed during the wood film production process. This

is followed by the cell walls collapsing. With a tensile strength of 469.9 MPa and a Young's modulus of 49.9 GPa, the film is strong in the fiber direction yet flexible[6].

- D. Zhao et al. reported that the cellulose offers a number of benefits, such as cheap cost, renewability, ease of processing, and biodegradability due to its natural biopolymer properties, in addition to its mechanical performance, dielectricity, piezoelectricity, and convertibility being attractive. Cellulose is widely employed as a substrate, binder, dielectric layer, gel electrolyte, and derived carbon material for flexible electronic devices due to its many benefits. The invention of improved functional materials using cellulose's benefits will have a major influence on portable intelligent devices[46].
  
- P. Tapsanit and J. Maitip reported that the technique of creating partially delignified wood (PDW) involved boiling natural wood measuring  $6 \times 6 \times 0.3 \text{ cm}^3$  in 30% w/v, 300 mL  $\text{H}_2\text{O}_2$  solution for 30 hours at a temperature of around  $78^\circ\text{C}$ . The wood was then freeze-dried. The original size and shape of the natural wood may be retained by the freeze-dried PDW. According to diffuse reflectance UV-Vis-NIR spectroscopy, the PDW's average solar absorptivity is 11%, which is around three times less than that of natural wood[47].
  
- M.M Oliveira et al. reported a novel one-pot synthesis is provided for the chemical production of graphene/polyaniline nanocomposites. Beginning with benzene and aniline, the process—which is based on chemical interactions at liquid-liquid interfaces—ends with nanocomposites, which are thin films of polyaniline combined with graphene. nanocomposites made with varying polymer/graphene ratios exhibit good pseudocapacitive behaviors (specific capacitance of  $267.2 \text{ F cm}^3$ )[48].
  
- Xi. Liu et al. fabricate a free-standing cellulose/GO/PANI composite aerogels by in-situ polymerization of aniline in the cellulose/GO three-dimensional frameworks. The cellulose/GO<sub>3.5</sub>/PANI electrode exhibits excellent electrochemical performances; at a current density of  $1.0 \text{ mA/cm}^3$ , it produced a maximum areal specific capacitance of  $1218 \text{ mF/cm}^2$  and retained good cycling stability, with capacitance retention of 83% after 1000



charge-discharge cycles. This provides a workable and effective way to make the ideal electrode materials for highly effective flexible energy storage systems [49].

- Z. Ahmed et al. synthesized a cellulose hydrogel/GO/PANI composite for supercapacitor applications. The ternary composite electrode demonstrated a real capacitance improvement of  $980 \text{ F g}^{-1}$  at 10 mV and greatly increased cycle stability, suggesting that cellulose hydrogel has a synergistic impact on PANI-GO[50].
- Yun Lu et al. reported a straightforward layer by layer (LbL) construction of PANI/CMWCNT and PANI/RGO composites on cellulose nanofibril (CNF) aerogels with a fibrillar porous network structure by drip and vacuum filtering in order to synthesis nanocomposite electrodes for high-capacity flexible supercapacitors. With 1 M aqueous  $\text{H}_2\text{SO}_4$  electrolyte, the specific capacitance of the CNF-[PANI/CMWCNT]10 (CPC10) and CNF-[PANI/RGO]10 (CPR10) electrodes are 965.80 and 780.64  $\text{F g}^{-1}$ , respectively[51].
- Supercapacitor CP electrodes showed high specific energies and quick capacitive response, but their low cycle stability prevented them from being used in more general applications. To reduce this barrier P. Dubey et al. generated a composite of human hair-derived activated carbon (HHAC) and polypyrrole (HHAC/PPy). When evaluated in 1 M  $\text{H}_2\text{SO}_4$ , the HHAC/PPy composite performs better than pure HHAC and PPy, yielding a higher specific capacitance of 358  $\text{F/g}$  at 0.5  $\text{A/g}$ , instead of 274 and 53  $\text{F/g}$  for the separate components. This composite has great potential for supercapacitor applications[52].
- S.K Nayak et al. fabricate polyaniline (PANI) and multiwalled carbon nanotubes (MWCNT) filled flexible porous mixed matrix membrane (MMM) using chitosan (CS) and cellulose acetate (CA) for use in supercapacitor applications. When compared to a paper-based electrode made of CA/CS (CC) with the same composition of PANI and MWCNT (15.71  $\text{mF/cm}^2$  at a scan rate of 25  $\text{mV/s}$ ), the results show that the MMM electrode's distinct membrane shape contributed to its improved areal capacitance of 30.69  $\text{mF/cm}^2$  at a scan rate of 25  $\text{mV/s}$ [53].

- Jiang et al. presented a novel method for growing *Gluconacetobacter hansenii* bacteria in the presence of GO flakes and poly(3,4-ethylenedioxythiophene)-poly(styrenesulfonate) (PEDOT-PSS) under aerobic and static growth conditions in order to create flexible and light weight bacterial nanocellulose (BNC/graphene oxide) based composite film electrodes. The resultant rGO/PEDOT-PSS/BNC composite electrode showed remarkable mechanical flexibility, allowing it to be twisted almost 180 degrees without any layer delamination[54].
- Hou et al. fabricated a sandwich-like film comprising carbon nanotubes (CNTs), nanofibrillated cellulose (NFC), and CNTs is made of both NFC and CNTs. Then, using the CNT/NFC/CNT film as the working electrode, Ag/AgCl as the reference electrode, and Pt foil as the counter electrode in a three-electrode electrolyzer, they electrodeposited a uniform PPy layer on the film to create a flexible PPy-CNT//NFC//PPy-CNT electrode. The resulting flexible electrode demonstrated a high specific capacitance of 11.25 F/cm<sup>3</sup>, a tensile strength of 60.8 MPa, and a high conductivity of 90.8 S/cm[55].
- J. Jiang et al. reported that in today's world, the use of portable electronic gadgets is growing quickly, requiring effective energy solutions. A potential option that serves as a transition between traditional batteries and rechargeable alternatives is the supercapacitor. Supercapacitors based on graphene and metal oxide have drawn interest due to their long cycle life and excellent power density. Their exceptional 2630 m<sup>3</sup>/g capacitance improves functioning. In order to increase conductivity during performance and create nanochannels for efficient electron conduction, activated carbon is used[56].
- C. Wang et al. reported that the development of supercapacitors depends heavily on metal oxide carbon nanosheet conducting polymers. When compared to their conventional equivalents, these supercapacitors have better properties, such as higher capacitance, power density, and energy density. They show amazing long-term stability with a pseudocapacitance of 236.5 F/g and an excellent long-term sustainability of 5000 cycles. The supercapacitors reach a greater potential of -0.4 V to -0.8 V in an aqueous KOH solution. Improved ion movement is made possible by the prepared material's enhanced

porosity. Many scientists are working to improve the electrodes of these supercapacitors in order to improve their electrochemical characteristics[57].

- J. Lin et al. reported that the conducting polymers more especially, polyaniline, or PANI along with metallic and carbonaceous elements have come to play a crucial role in energy conversion and storage systems. PANI has great potential in supercapacitor applications because of its high specific capacitance, versatility, and affordability. It is a material that may be used on its own to fabricate electrodes. However, PANI's limited applicability stems from its intrinsic stability issues. To get over these restrictions and improve performance overall, combining PANI with other active materials like metal compounds, carbon materials, or other polymers works well[58].
- Y Han and L Dai reported that the Poly-aniline's structure and configuration greatly affect its specific surface area and ion diffusivity, which in turn affects how it behaves under redox conditions. PANI shows an experimental specific capacitance in H<sub>2</sub>SO<sub>4</sub>-based electrolytes that ranges from 200 to 550 F/g in a potential window of around 0.8 V. Because of their excellent conductivity and low cost, conducting polymers are frequently used as the electrode material in supercapacitors. These substances allow for redox processes to occur quickly and reversibly, which makes it easier to store charges with a high density and produce a high faradic capacitance. However, after several cycles of charging and discharging, conducting polymers' natural swelling and shrinking during electrochemical redox reactions can result in a shortened cyclic life and capacitance loss [59].
- Li Dong et al. synthesized a polyaniline@MnO<sub>2</sub>/graphene composite by two step method. Electrochemical analyses indicate that electrodes made of nanostructured PMGNs have improved reversible capacitance, which reaches 695 F/g at a high current density of 4 A/g even after 1000 cycles. When used as supercapacitor electrode materials, the ternary composites show better electrochemical capacitance than each isolated component. The combined effects of MnO<sub>2</sub>, PANI, and graphene are largely responsible for this impressive electrochemical performance[60].

- W. Wei et al. successfully fabricate composite films made of reduced graphene oxide, carbon nanoparticles, and polyaniline (RGO/CNs/PANI) by electrodepositing PANI onto a composite film of RGO/CNs. This composite film contributes to improved electrochemical performance by acting as a highly conductive support with exceptional tensile strength. As prepared film of RGO/CNs/PANI-2 demonstrated a very good specific capacitance of 564.0 F/g at a current density of 10 A/g and 787.3 F/g at a current density of 1 A/g. Furthermore, the film exhibited exceptional cycling stability, retaining over 90% of its capacitance even after 2000 CV cycles. The RGO/CNs/PANI film electrodes with superior properties hold great promise as free-standing, binder-free paper-like film electrodes for high-performance supercapacitor[61].
  
- M. Rafat et al. synthesized Activated carbon (AC) from rotted carrots, chemically activated with  $\text{ZnCl}_2$ , was thoroughly investigated to see how activation temperature affected its porosity. Aqueous electrolytes showed better specific capacitance ( $135.5 \text{ F g}^{-1}$  at 10 mHz) in electrochemical evaluations, while ionic liquid electrolytes had the highest specific energy ( $29.1 \text{ Wh kg}^{-1}$  at  $2.2 \text{ A g}^{-1}$ ) and specific power ( $142.5 \text{ kW kg}^{-1}$  at  $2.2 \text{ A g}^{-1}$ ) in electrochemical tests. These results highlight the promise of the environmentally benign and reasonably priced AC-based electrode for energy storage applications[62].
  
- Yan Yan et al. revealed the effective synthesis of materials based on carbon and nickel oxide for use in supercapacitors. The mixture of nickel oxide and carbon exhibited capacitance values of 823 and 988 F/g, whereas retention over 5000 cycles of 96.5%. The supercapacitor material composed of nickel oxide and activated carbons demonstrated a capacitance of  $230 \text{ mF cm}^{-2}$ , and after 5000 cycles, the capacitance retention value was 92.8%. The supercapacitor device's highest power density is stated to be  $231.2 \text{ mW cm}^{-2}$ , while its realized energy density is  $4.18 \text{ mWh cm}^{-3}$ [63].

## **Chapter 3**

### **Experimental and Characterizations**

The preparation of materials and the methods used for their analysis are explained in this chapter.

### 3.1 Materials

Balsa wood strips (2cmx7cm) was purchased from China, Sodium hydroxide (NaOH), Sodium sulphite ( $\text{Na}_2\text{SO}_3$ ), Hydrogen peroxide ( $\text{H}_2\text{O}_2$ , 34.5-36.5%), Ethanol ( $\text{CH}_3\text{CH}_2\text{OH}$ , 99.8%), Graphite powder, Sulphuric acid ( $\text{H}_2\text{SO}_4$ , 98%), Potassium permanganate ( $\text{KMnO}_4$ , 99-100.5%), Hydrochloric acid (HCl, 37%), Aniline monomer (ANI), Potassium persulfate (KPS), all the chemical were purchased from Sigma Aldrich. In every experiment, deionized water (DI) was used.

### 3.2 Synthesis of GO

A modified version of Hummer's process was used to synthesize graphite powder into GO[64]. To sum up, room temperature first, 50 mL of pure  $\text{H}_2\text{SO}_4$  was mixed with 1.0 g of graphite powder. There was an ice bath to cool the mixture to  $5^\circ\text{C}$  while stirring, and the mixture's temperature was maintained below  $5^\circ\text{C}$  for 30 minutes. To create a uniform mixture,  $\text{KMnO}_4$  (4.0 g) was then gradually added while stirring and then cooled down to prevent the mixture's temperature from rising over  $10^\circ\text{C}$ . diluted the liquid further to 150 mL of distilled water by adding 50 mL of distilled water and stirring it for two hours at room temperature. In order to minimize the remaining  $\text{KMnO}_4$  in the reaction mixture, 10 mL of 30%  $\text{H}_2\text{O}_2$  was added while the mixture was being stirred continuously. This caused the color to shift to bright yellow. After filtering, the solid was repeatedly cleaned with 400 mL of 5% aqueous HCl to eliminate metal ions, and then it was treated with distilled water until pH 6 was reached. After that, the resultant graphite oxide was subjected to the oven drying process. The final GO, which had been in powder form, was characterized.

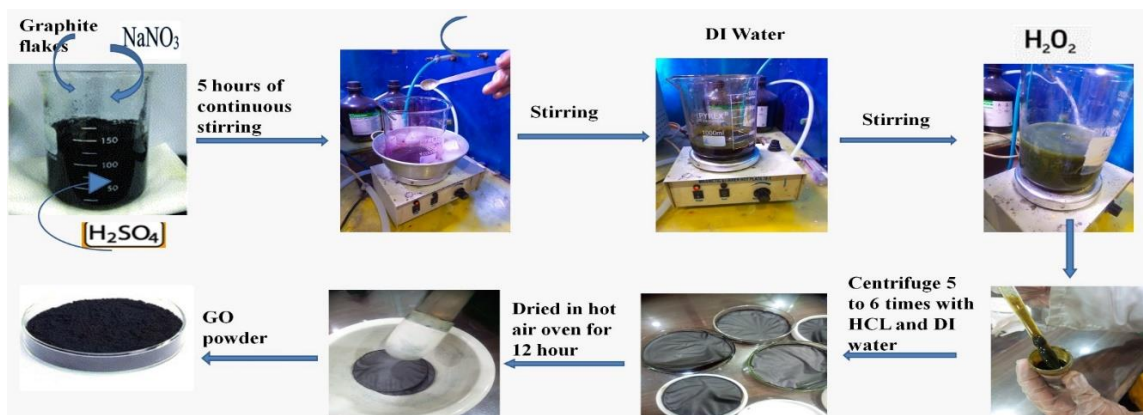


**Fig 3.1** Synthesis of Graphene Oxide (GO)

### 3.3 Delignification of wood

Firstly, we take Balsa wood and cut into slices then wood slices add into a solution of NaOH and Na<sub>2</sub>SO<sub>3</sub>. After submerging wood slices in a mixture of NaOH and Na<sub>2</sub>SO<sub>3</sub>, they were immediately placed inside a vacuum chamber. The liquid was allowed to enter the wood lumina by means of vacuum. Following that, wood pieces were submerged in the H<sub>2</sub>O<sub>2</sub> solution and boiled until they became transparent. To eliminate the chemicals, boiling DI water was used to submerge the chemically treated wood many times. After that, treated wood slices were let to dry in open air to create the ultimate super-flexible wood membrane[65].



**Fig 3.2** Delignification of Balsa wood



**Fig 3.3** Practical demonstration of mechanical strength and flexibility for FBW

### 3.4 Synthesis of flexible electrode of balsa wood/GO/PANI

Precisely, GO powder was added into 10ml of 1M HCl solution and ultrasonicated for half an hour to gain a uniform dispersion. Wood slices are added into GO solution and the solution was filled into the pores of the wood by vacuum impregnation for 30 to 45 minutes. After that 2ml aniline added into above solution. The oxidant solution was prepared by dissolving KPS into 10ml of 1M HCl. Then the mixture of wood GO and aniline are added into the oxidant solution and the greenish liquid is stirred for one hour. Then put the solution for 6 hours at room temperature. The aniline could be oxidized and polymerized into PANI to obtain wood/PANI/GO electrode. The polyaniline and GO composite form a uniform layer on the chip on balsa wood. After being cleaned up to remove superfluous potassium persulfate Wood/PANI/GO dry for 5 hours at 60°C. Final wood/PANI/GO electrode were characterized.

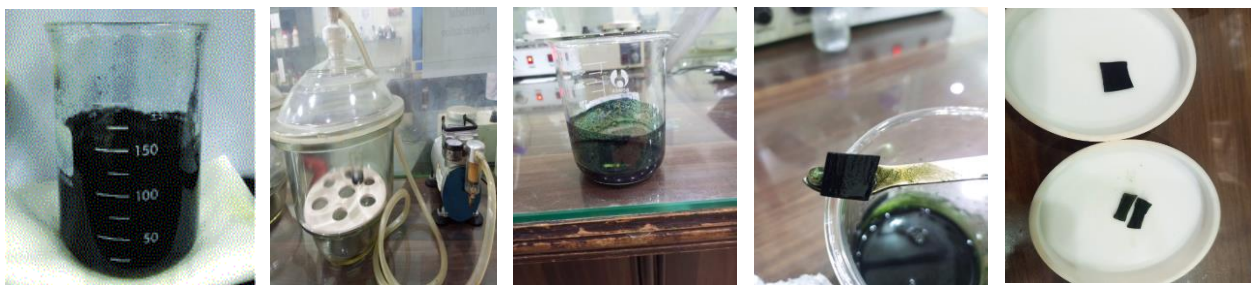


Fig 3.4 Synthesis of flexible electrode of balsa wood/GO/PANI

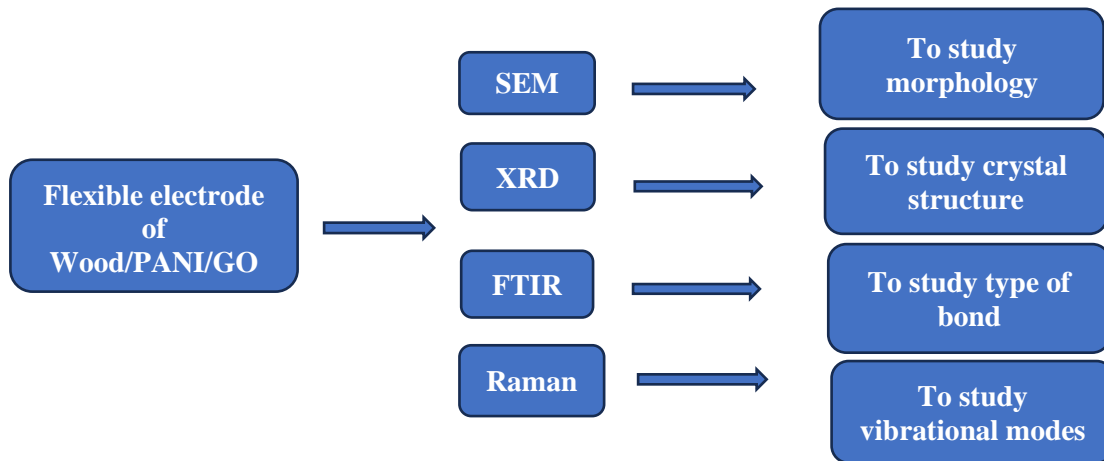


Fig 3.5 Flexibility of Balsa wood after polymerization is retained



### 3.5 Characterizations

Different approaches are proposed to explore the chemical and physical properties of the manufactured materials. The morphology and structure of wood were characterized by a scanning electron microscope (SEM) and the distribution of GO and PANI in wood was characterized by Energy Dispersive Spectroscopy (EDS). X-ray diffraction (XRD) was used to investigate the structural characteristics of composites. For the investigation of various bond types in graphene and its composite materials, Fourier Transform Infrared Spectroscopy (FTIR) should be employed. Materials are characterized using Raman spectroscopy, which looks at the vibrational modes of molecular bonds to reveal information about their structural makeup.



**Fig 3.6** Technique for characterizing materials that is suggested to investigate their chemical and physical characteristics

### 3.6 Electrochemical properties

It is proposed that the materials be evaluated using a potentiostat in order to determine the electrochemical performance for supercapacitor applications. Cyclic voltammetry (CV) for measuring capacitance, Galvanostatic Charge/Discharge Cycle (GCD) for evaluating charge/discharge characteristics, and Electrochemical Impedance Spectroscopy (EIS) for measuring resistance are the three main parameters that are particularly important for study. A commonly used method in supercapacitor research is cyclic voltammetry (CV), which separates faradaic and non-faradaic processes to clarify electrochemical properties. This qualitative examination shows the redox potentials of the electrode materials and aids in the identification of

supercapacitor kinds. The potentiostatic test reveals current peaks that indicate oxidation and reduction processes within a designated potential window by applying a succession of voltages.

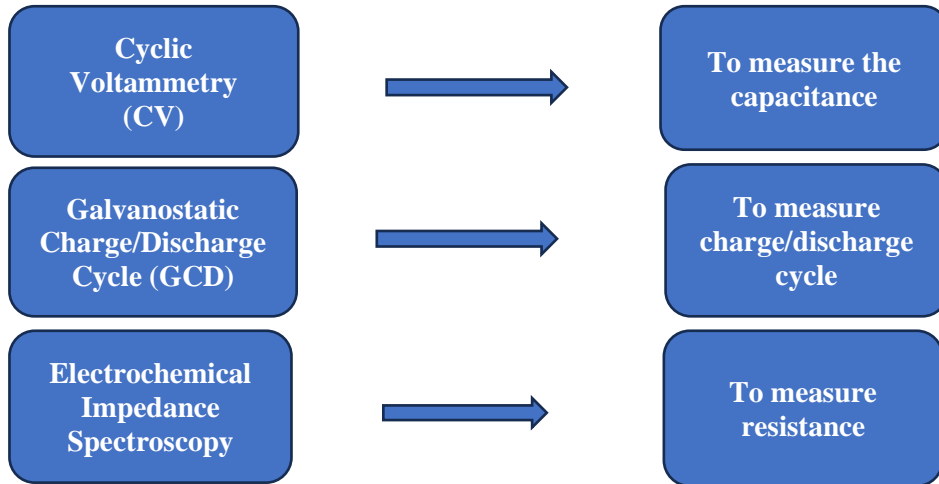


**Fig 3.7** An overview of the suggested plan to examine the material used in supercapacitors to investigate its electrochemical performance

A common technique for evaluating the performance of energy storage devices, especially supercapacitors, in both potentiostatic and galvanostatic modes is cyclic charge-discharge (CCD). In both symmetric and asymmetric electrode systems, the galvanostatic mode allows for the measurement of specific capacitance, energy density, and power density since potential is measured at a constant current during scanning. It is also possible to investigate the charge-discharge cycle over time.

Electrochemical impedance spectroscopy, or EIS, is used to examine a system's electrical behavior across a variety of frequencies. When it comes to supercapacitors, EIS offers important information on the electrochemical interface's capacitance, resistance, and impedance. This information helps with a thorough analysis of the behavior and performance of the device.

## **Chapter 4**

### **Results and Discussions**

## 4.1 Characterizations

Fourier Transform Infrared spectrum (FT-IR) is used to check the occurrence of functional groups in synthesized materials in a range of  $4000\text{--}400\text{ cm}^{-1}$  using KBr pellets. The morphology and structure of wood were characterized by a scanning electron microscope (SEM), the distribution of GO and PANI in wood was characterized by Energy Dispersive Spectroscopy (EDS). To determine crystal structure, X-ray Diffraction (XRD) measurements are carried out by X-ray powder diffractometer. The sample were scanned from  $2\theta = 5^\circ - 60^\circ$  at a scanning speed of  $5^\circ/\text{min}$  with a step width of  $0.04^\circ$ . The Raman spectra were recorded by using the He-Ne laser beam with a wave length of  $532\text{nm}$ .

### 4.1.1 Scanning Electron Microscopy

The primary components of balsa wood are cellulose, hemicellulose, and lignin. While lignin is a three-dimensional amorphous polyphenolic macromolecule made up of three different kinds of phenyl propane units that combine to produce a complex, highly branching, and amorphous structure, cellulose and hemicellulose are polysaccharides. The compounds' local repartition was non-uniform. The majority of the lignin was found on the fiber's surface, with cellulose making up the majority of the backbone. Of the overall lignin content, the intercellular layer made about  $3/4$  and the secondary wall the remaining  $1/4$ [66]. The chromophoric groups remove upon delignification with  $\text{Na}_2\text{SO}_3$ , causing the resulting scaffold to become white in color. The layer of cell walls gets thinner in thickness. The removal of the middle lamella and the lignin-rich primary wall causes alterations in the Balsa wood's hierarchically organized cell walls. An enhanced porosity can be explained by thin wall constructions with expanding pits. The morphology of the balsa wood sample free of lignin was significantly impacted by the further removal of hemicellulose using a  $\text{NaOH}$  solution[67]. Delignification produces ultra-high flexibility and exceptional mechanical strength by increasing surface area through micropores while decreasing macropores to improve scaffold density as shown in fig 4.1. The wood becomes highly hydrophilic with aligned cellulose structure and free OH groups as a result of the delignification process. Because of its hierarchically aligned cellulose structure and free reactive OH groups, DW can be employed as a bio template to create a variety of functional materials.

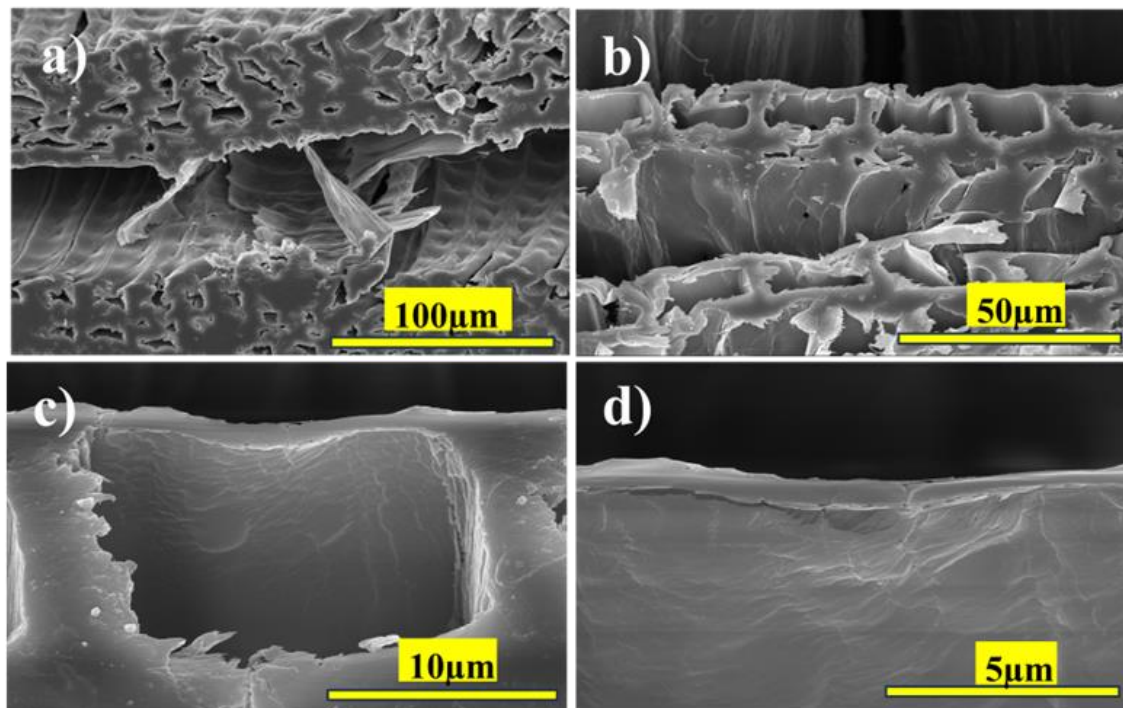


**Fig 4.1** SEM images of delignified balsa wood

#### 4.1.2 Fourier Transform Infrared Spectroscopy of graphite, GO, and rGO

FTIR spectra of graphite, GO, and RGO are shown in Figure. FTIR was employed to look at the existence of vibrational (transmittance/absorption) spectra recorded, which reveal the functional groups present in the materials. This research is predicated on the idea that molecular bonds are vibrationally excited when infrared light energy is absorbed[68], within the wavelength from 4000 to 400  $\text{cm}^{-1}$ . After the oxidation process, more oxygen-containing functional groups should be present in GO, the oxide form of graphite. Nonetheless, RGO is predicted to have a negligible quantity of functional groups that include oxygen during reduction.

Graphite did not exhibit a notable peak in Figure 4.2[69]. However, with GO, the extensive and rigorous peaks are appeared. The main characteristic peaks located at 1020  $\text{cm}^{-1}$  C-O (epoxy group) were due to C-O-C stretching vibration[70], whereas the peak at 1380  $\text{cm}^{-1}$  are related to C-OH stretching vibration[71], C=O stretching ( $-\text{COOH}$  group) was shown at 1620  $\text{cm}^{-1}$ . The peak in the region around 3000 to 3500  $\text{cm}^{-1}$  is responsible for the stretching vibration of hydroxyl group. Since all of these carboxylic, epoxide, carbonyl and hydroxyl groups were present, it was determined that oxygen (O) molecules were heavily occupied at the GO's edge and basal plane, indicating that the synthesis of GO was successful[72].

In comparison to GO, the peaks for RGO became less wide, indicating a considerable removal of the hydroxyl group. It is also evident that additional peaks in the FTIR spectra of GO became less strong than those peaks at the same position. These peaks were similarly caused by the elimination of oxygen during the reduction process by employing hydrazine hydrate[73]. As a result, only small quantities of functional group residue are still present at the edge and basal plane of RGO after the oxygen-containing functional groups were effectively partly eliminated.

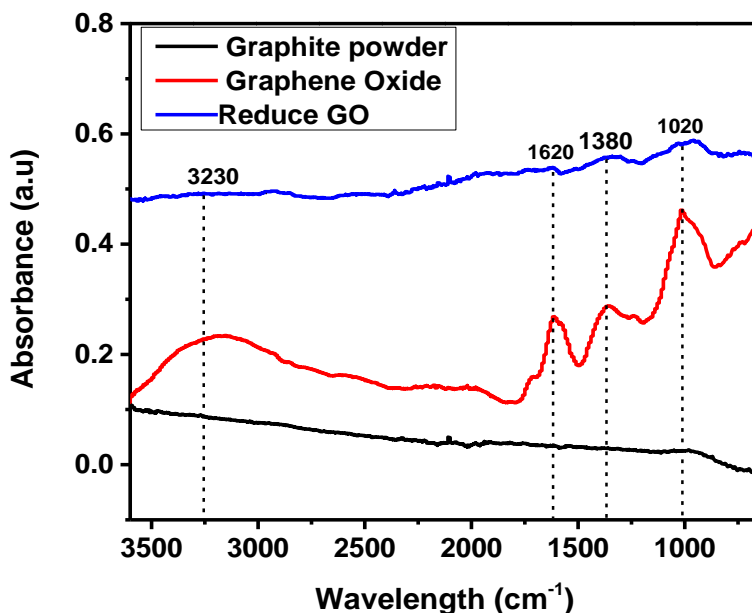


Fig 4.2 FTIR spectrum of a) Graphite powder b) Graphene oxide c) Reduce Graphene oxide

#### 4.1.3 Fourier Transform Infrared Spectroscopy of BW/GO/PANI

Figure 4.3 shows the FTIR spectroscopy-measured absorption spectra of the delignified balsa wood (DBW) and natural balsa wood in the wavenumber range of 4000 – 400  $\text{cm}^{-1}$ . The wavelength 1025  $\text{cm}^{-1}$ , corresponds to the greatest absorption peak of natural wood and is located in the atmospheric windows. The absorption peak originates from the stretching vibration of the C-O bond, which joins the C atom and OH group in the cellulose glucose ring [74]. The C-O vibration of the syringyl ring in lignin molecules is linked to the peak location at 1235  $\text{cm}^{-1}$ [74]. The lignin molecules' C=O stretching vibration is the source of the peak location at 1730  $\text{cm}^{-1}$ [74]. Following the delignification procedure, certain peak positions are removed and some peak positions with decreasing absorbance are left.

After the delignification process, FTIR spectroscopy verifies that lignin molecules are eliminated and modified, and the strong emission peaks resulting from the cellulose molecules' molecular vibrations in the DBW emerge[47].

Furthermore, the DBW sample's absorption peak, which was caused by the stretching vibration of the OH groups, is shifted to 3342  $\text{cm}^{-1}$  in the BW/GO/PANI sample, indicating a strong hydrogen bonding interaction between the three components[49].

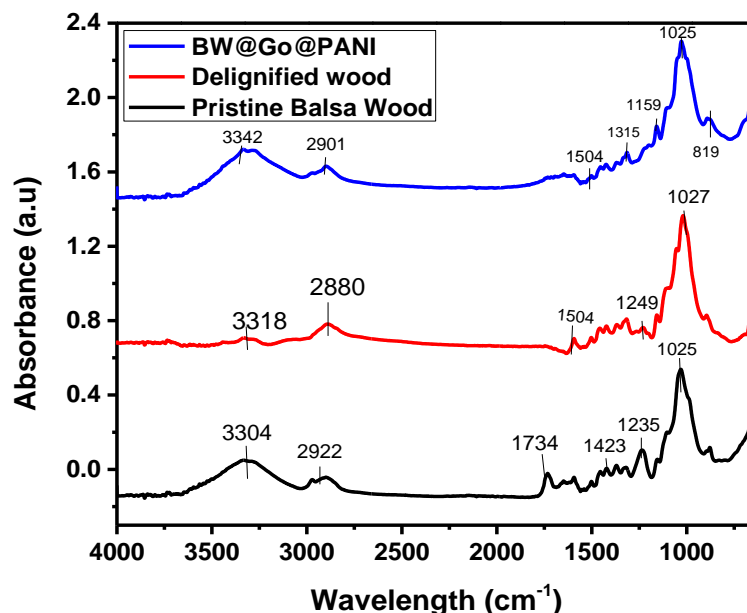


**Fig 4.3** FTIR spectrum of Pristine balsa wood, Delignified balsa wood, and Synthesized B/GO/PANI flexible electrode

#### 4.1.4 Raman Spectroscopy

The Raman spectroscopy technique is frequently used to determine the vibrational modes of molecules, but it may also be used to find low-frequency rotational and other modes in systems. Raman spectroscopy is widely used in chemistry to produce a structural fingerprint that makes it possible to identify compounds. The intensity, or count rate, is usually plotted on the y-axis and the frequency of the Raman shift is plotted on the x-axis when plotting a Raman spectrum. The ternary composite's structural features were reflected by the application of Raman spectroscopy. Fig 4.4 shows the Raman spectra of the composite of balsa wood BW/GO/PANI. Following collaboration with PANI, the BW/GO/PANI composite exhibited mostly characteristic bands at approximately 1354 and 1585  $\text{cm}^{-1}$ , corresponding to the C–N/C=N and C–C bonds, respectively.

This indicates that PANI has been effectively prepared and introduced[49][75]. The BW/GO/PANI sample's spectrum shows peaks at 1354 and 1585  $\text{cm}^{-1}$ , which indicate the presence of a  $\pi$ - $\pi$  interaction between the conjugated structure of the PANI and the GO. This interaction would enhance the materials' electrical conductivity [76][77].

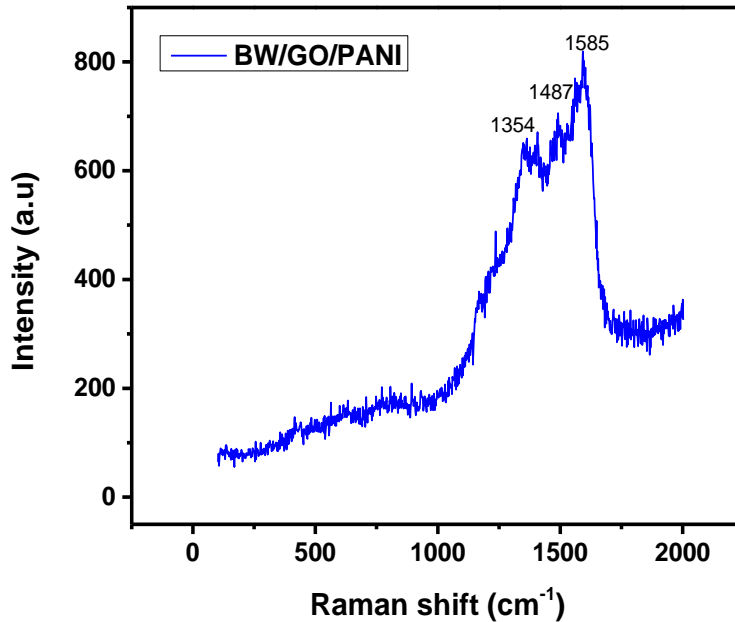


Fig 4.4 Raman spectroscopy of BW/GO/PANI flexible electrode

## 4.2 Electrochemical Performance

Cyclic voltammetry (CV) is a powerful and popular electrochemical technique for investigating the reduction and oxidation processes of molecular species. Studying chemical processes involving electron transport, such as catalysis, is made much easier using CV [78]. Cyclic Voltammetry is rarely used for quantitative determination but widely used for the study of redox reaction, for understanding intermediate and for obtaining stability of reaction. The specific capacitances were determined from CV using the following [79] equation.

$$C_{sp} = \frac{\int I \times dV}{v \times m \times \Delta V} \quad (4.1)$$

In this formula, the specific capacitance (F/g), discharge current (A), potential range (V), scan rate (V/s), and total mass (g) of the electrode active materials are all represented by Csp [78].



Constant current density values, such as 0.07, 0.08, 0.09, 0.1, and 0.5 mA/g, were used for GCD measurements. The following formula were used to get the areal specific capacitance ( $C_s$  in mF  $\text{cm}^{-2}$ ) using the GCD approach[80][81].

$$C_s = \frac{I \times \Delta t}{S \times \Delta V} \quad (4.2)$$

where  $\Delta V$  is the potential window of the discharge curve excluding the initial drop (V),  $S$  is the area of the electrode ( $\text{cm}^2$ ),  $t$  is the discharge period (s), and  $I$  is the charge-discharge current (mA). The following equations were used to compute the areal specific capacitance ( $C_a$  in mF  $\text{cm}^{-2}$ ), energy density ( $E_a$  in  $\mu\text{W h cm}^{-2}$ ), and power density ( $P_a$  in  $\mu\text{W cm}^{-2}$ ) for the symmetric supercapacitor device[80][81].

Nyquist, Bode-phase, Bode-magnitude, and admittance plots were created using impedance data collected for electrochemical impedance spectroscopy (EIS) experiments. For the purpose of developing a two-electrode supercapacitor system in a 1 M  $\text{H}_2\text{SO}_4$  solution at the open circuit potential, Using the Iviumstat model potentiostat/galvanostat, EIS measurements were performed. They are carried out across a wide frequency range (10 mHz–100 kHz) with a modest voltage amplitude of 10 mV[82].

### **CV measurements**

The electrochemical properties of the BW/GO/PANI sample were studied through CV measurement. in 1 M  $\text{H}_2\text{SO}_4$  aqueous electrolyte using a three-electrode test. The material produced by in situ polymerization served as a working electrode, a platinum electrode as the counter- electrode, and a AgCl/Ag electrode as the reference electrode. Measurements of the CV curves were made in the potential of  $-0.2$  to  $0.8$  V at scan rates of 10, 20, 30, and 40  $\text{mV s}^{-1}$ .

The reversible electrode reaction's extent may be ascertained based on the curve forms [77]. The BW/GO/PANI electrode is more reversible and has a higher integrated CV area. The peak current density rises with an increase in scan rate, causing the anodic peaks to shift to lower values and the cathodic peaks to move right to higher voltages in the CV curves [76].

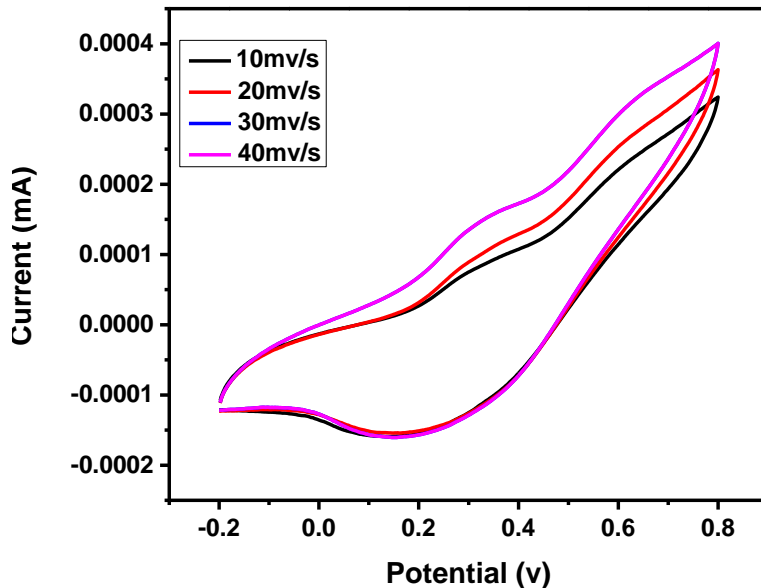


Fig 4.5 CV curves of BW/GO/PANI at different scan rates

### GCD measurements

To examine the cycling stability of the BW/GO/PANI flexible electrode galvanostatic cycling tests were carried out. The charge-discharge studies were performed at 0.07, 0.08, 0.09, 0.1, and 0.5 mA in 1M H<sub>2</sub>SO<sub>4</sub> solution. Equation (4.2) was utilized to compute the discharge capacitance based on the linear portion of the discharge curve. [83][84]. The highest specific capacitance was obtained as  $C_{sp}=343 \text{ mF/cm}^2$  at current density of 0.5 mA for BW/GO/PANI flexible electrode. The shape and specific surface area of the synthesized BW/GO/PANI flexible electrode determine its electrochemical capacitance. Because the composite material's features increase the contact area between the electrode and the electrolyte, they would enhance the surface adsorption/desorption process in the presence of H<sub>2</sub>SO<sub>4</sub> solution. It's critical to maintain high capacitance during high charge/discharge for commercial applications.

In discharge step, the GCD curves may be split into two halves with distinct slopes: The initial segment at high potential in the potential windows displays the less common electrical double layer capacitance behavior, whereas the second half with a lower slope displays the most significant faradaic battery-like behavior. At the beginning of each discharging phase, there may be a little IR decrease caused by bulk solution resistance, ion-migration resistance, and electrode

material electronic resistance. The power and energy densities of the charge storage device may suffer as a result [85].

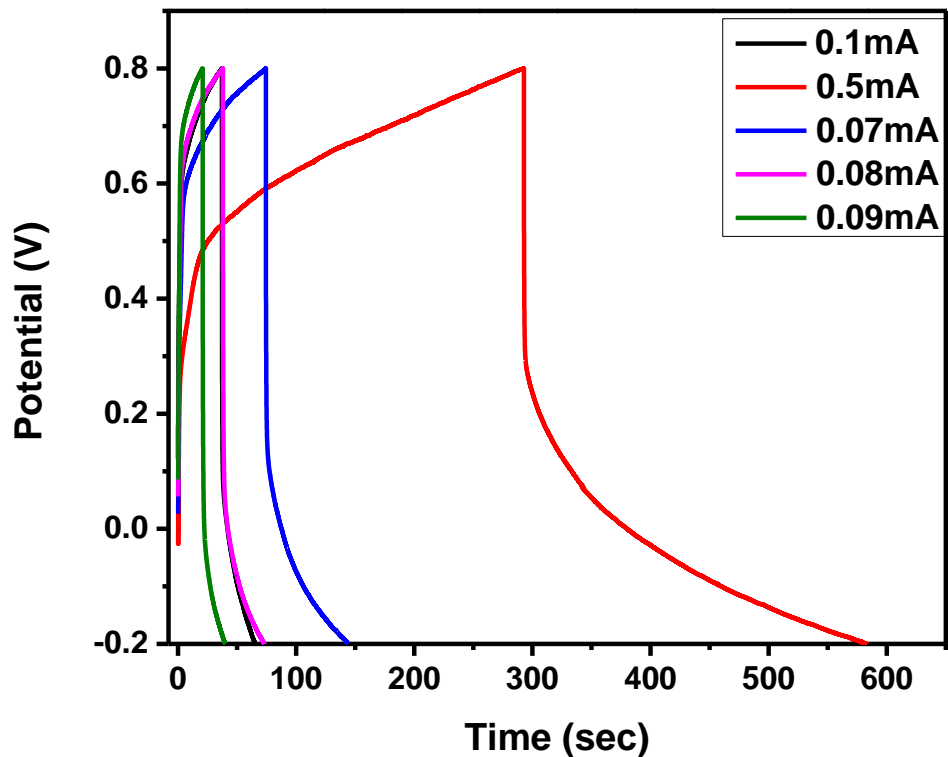


Fig 4.6 GCD curves of BW/GO/PANI at different current densities

### EIS measurements

The concept of impedance can be understood if we suppose it as the analog of resistance in a DC, direct current system. When we apply an oscillating voltage to measure the oscillating current response and this oscillating voltage which oscillates at an angular frequency of  $\omega$  with the current response of similar angular frequency but it can also have a different phase shift  $\theta$  which is caused by reactants supposed as capacitors or inductors within given current. EIS models provide insight into ionic and electronic transport as well as the mechanisms underlying material degradation in energy storage. The interactions at the interface between an electrode and an electrolyte are explained by the EIS.

The BW/GO/PANI composites' specific capacitances were determined using Nyquist plots in a 1 M H<sub>2</sub>SO<sub>4</sub> solution. The actual component of the calculation was the impedance and resistance measurements, while the capacitance was determined using the formula (Eq. 4.3) [86].

$$C_{sp} = -1 / (2\pi \times f \times Z'') \quad (4.3)$$

in this formula,  $\pi = 3.14$ ,  $f$  is the frequency in Hz, and  $-Z''$  is the imaginary part of the impedance. A semicircle illustrates the kinetics of electron transport during a redox reaction at the interface between the electrolyte and electrode material. On the other hand, the linear portion explains how ionic mass diffusion or a carriage process occurs [87]. Higher capacitance is the result of decreased ionic mass diffusion or a carriage process occurs [87]. Higher capacitance is the result of decreased ion transfer resistance and decreased charge density in the electrolyte [88]. The slope of the curve in the lower frequency region represents the diffusive resistance of ion transport in the electrolyte to the SS electrode, also known as Warburg resistance [89]. As we shown in the fig the steeper line for BW/GO/PANI electrode indicates a faster ion diffusion process, as reflected by lower resistance ( $R_s$ ) [38]. Plots indicate a tiny semicircle in the high-frequency range and an angled line in the low-frequency zone.

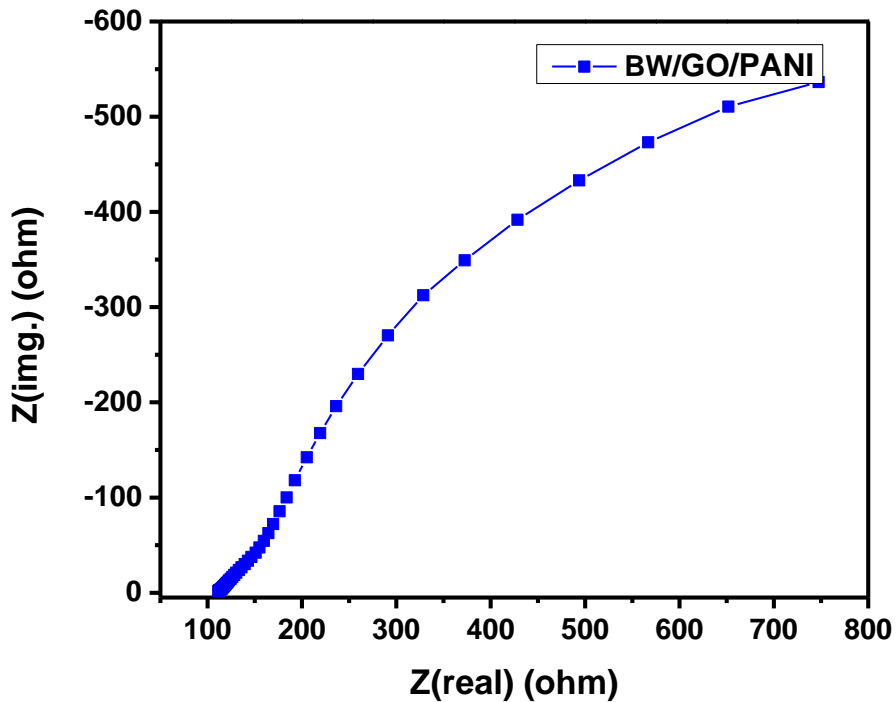


Fig 4.7 EIS performance of BW/GO/PANI flexible electrode

## **5. Conclusion**

Balsa wood/GO/PANI flexible electrode material can be carefully produced using aniline's in-situ polymerization in the delignified balsa wood/GO three-dimensional frameworks. When no additional binders are present, balsa wood, GO, and PANI can be used as electrode materials because of their considerable flexibility and capacity for significant bending. The balsa wood/GO/PANI electrode has excellent electrochemical performances; at a current density of 0.5 mA/cm<sup>2</sup>, it produced a maximum areal specific capacitance of 343 mF/cm<sup>2</sup>. Our research offers a technique based on transparent CNFs paper for creating hybrid electrodes with various microstructures for upcoming flexible supercapacitors.

## Reference

- [1] P. C. Slorach, H. K. Jeswani, R. Cuéllar-Franca, and A. Azapagic, “Energy demand and carbon footprint of treating household food waste compared to its prevention,” *Energy Procedia*, vol. 161, no. 2018, pp. 17–23, 2019, doi: 10.1016/j.egypro.2019.02.053.
- [2] K. K. Jaiswal *et al.*, “Renewable and sustainable clean energy development and impact on social, economic, and environmental health,” *Energy Nexus*, vol. 7, no. April, p. 100118, 2022, doi: 10.1016/j.nexus.2022.100118.
- [3] F. Jiang *et al.*, “Wood-Based Nanotechnologies toward Sustainability,” *Adv. Mater.*, vol. 30, no. 1, pp. 1–39, 2018, doi: 10.1002/adma.201703453.
- [4] C. Chen and L. Hu, “Nanocellulose toward Advanced Energy Storage Devices: Structure and Electrochemistry,” *Acc. Chem. Res.*, vol. 51, no. 12, pp. 3154–3165, 2018, doi: 10.1021/acs.accounts.8b00391.
- [5] J. Huang *et al.*, “Wood-Derived Materials for Advanced Electrochemical Energy Storage Devices,” *Adv. Funct. Mater.*, vol. 29, no. 31, pp. 1–23, 2019, doi: 10.1002/adfm.201902255.
- [6] Q. Fu, Y. Chen, and M. Sorieul, “Wood-Based Flexible Electronics,” *ACS Nano*, vol. 14, no. 3, pp. 3528–3538, 2020, doi: 10.1021/acsnano.9b09817.
- [7] H. Kelly-Holmes, “Advertising as multilingual communication,” *Advert. as Multiling. Commun.*, vol. 45, pp. 1–206, 2016, doi: 10.1057/9780230503014.
- [8] A. Burk, “Ultracapacitors: why, how, and where is the technology,” *J. Power Sources*, vol. 91, no. 1, pp. 37–50, 2000.
- [9] J. R. Miller and P. Simon, “Materials science: Electrochemical capacitors for energy management,” *Science (80-. )*, vol. 321, no. 5889, pp. 651–652, 2008, doi: 10.1126/science.1158736.
- [10] A. S. Talhar and S. B. Bodkhe, “The global survey of the electrical energy distribution system: A review,” *Int. J. Electr. Comput. Eng.*, vol. 9, no. 4, pp. 2247–2255, 2019, doi: 10.11591/ijece.v9i4.pp2247-2255.
- [11] E. J. Cairns, “Batteries, Overview,” vol. 1, no. 1, pp. 117–126, 2004.
- [12] A. R. Dehghani-Sanij, E. Tharumalingam, M. B. Dusseault, and R. Fraser, “Study of energy storage systems and environmental challenges of batteries,” *Renew. Sustain. Energy Rev.*, vol. 104, no. January, pp. 192–208, 2019, doi: 10.1016/j.rser.2019.01.023.
- [13] M. Jayalakshmi and K. Balasubramanian, “Simple capacitors to supercapacitors - An overview,” *Int. J. Electrochem. Sci.*, vol. 3, no. 11, pp. 1196–1217, 2008, doi: 10.1016/s1452-3981(23)15517-9.
- [14] J. Ho, T. R. Jow, and S. Boggs, “Historical introduction to capacitor technology,” *IEEE Electr. Insul. Mag.*, vol. 26, no. 1, pp. 20–25, 2010, doi: 10.1109/MEI.2010.5383924.
- [15] J. Both, “The modern era of aluminum electrolytic capacitors,” *IEEE Electr. Insul. Mag.*,

- vol. 31, no. 4, pp. 24–33, 2015, doi: 10.1109/MEI.2015.7126071.
- [16] A. Noori, M. F. El-Kady, M. S. Rahmanifar, R. B. Kaner, and M. F. Mousavi, “Towards establishing standard performance metrics for batteries, supercapacitors and beyond,” *Chem. Soc. Rev.*, vol. 48, no. 5, pp. 1272–1341, 2019, doi: 10.1039/c8cs00581h.
- [17] M. Pershaanaa, S. Bashir, S. Ramesh, and K. Ramesh, “Every bite of Supercap: A brief review on construction and enhancement of supercapacitor,” *J. Energy Storage*, vol. 50, no. April, p. 104599, 2022, doi: 10.1016/j.est.2022.104599.
- [18] S. Rashidi, J. A. Esfahani, and F. Hormozi, “Classifications of Porous Materials for Energy Applications,” *Encycl. Smart Mater.*, pp. 774–785, 2021, doi: 10.1016/B978-0-12-803581-8.11739-4.
- [19] R. Chen, M. Yu, R. P. Sahu, I. K. Puri, and I. Zhitomirsky, “The Development of Pseudocapacitor Electrodes and Devices with High Active Mass Loading,” *Adv. Energy Mater.*, vol. 10, no. 20, pp. 1–33, 2020, doi: 10.1002/aenm.201903848.
- [20] A. Muzaffar, M. B. Ahamed, K. Deshmukh, and J. Thirumalai, “A review on recent advances in hybrid supercapacitors: Design, fabrication and applications,” *Renew. Sustain. Energy Rev.*, vol. 101, no. July 2018, pp. 123–145, 2019, doi: 10.1016/j.rser.2018.10.026.
- [21] R. Henríquez, A. S. Mestra-Acosta, E. Muñoz, P. Grez, E. Navarrete-Astorga, and E. A. Dalchiele, “High-performance asymmetric supercapacitor based on CdCO<sub>3</sub>/CdO/Co<sub>3</sub>O<sub>4</sub> composite supported on Ni foam,” *RSC Adv.*, vol. 11, no. 50, pp. 31557–31565, 2021, doi: 10.1039/d1ra05243h.
- [22] P. Asen, S. Shahrokhian, and A. I. Zad, “Transition metal ions-doped polyaniline/graphene oxide nanostructure as high performance electrode for supercapacitor applications,” *J. Solid State Electrochem.*, vol. 22, no. 4, pp. 983–996, 2018, doi: 10.1007/s10008-017-3831-9.
- [23] J. Zhang, Y. Cui, and G. Shan, “Metal oxide nanomaterials for pseudocapacitors,” 2019, [Online]. Available: <http://arxiv.org/abs/1905.01766>
- [24] Y. Wang *et al.*, “Recent progress in carbon-based materials for supercapacitor electrodes: a review,” *J. Mater. Sci.*, vol. 56, no. 1, pp. 173–200, 2021, doi: 10.1007/s10853-020-05157-6.
- [25] Q. Meng, K. Cai, Y. Chen, and L. Chen, “Research progress on conducting polymer based supercapacitor electrode materials,” *Nano Energy*, vol. 36, no. April, pp. 268–285, 2017, doi: 10.1016/j.nanoen.2017.04.040.
- [26] M. Ates and C. Fernandez, “Ruthenium oxide–carbon-based nanofiller-reinforced conducting polymer nanocomposites and their supercapacitor applications,” *Polym. Bull.*, vol. 76, no. 5, pp. 2601–2619, 2019, doi: 10.1007/s00289-018-2492-x.
- [27] M. H. A. Kudus, M. R. Zakaria, H. M. Akil, F. Ullah, and F. Javed, “Oxidation of graphene via a simplified Hummers’ method for graphene-diamine colloid production,” *J. King Saud Univ. - Sci.*, vol. 32, no. 1, pp. 910–913, 2020, doi: 10.1016/j.jksus.2019.05.002.

- [28] S. Sarma, S. C. Ray, and A. M. Strydom, “Electronic and magnetic properties of nitrogen functionalized graphene-oxide,” *Diam. Relat. Mater.*, vol. 79, no. August, pp. 1–6, 2017, doi: 10.1016/j.diamond.2017.08.011.
- [29] B. Xu *et al.*, “What is the choice for supercapacitors: Graphene or graphene oxide?,” *Energy Environ. Sci.*, vol. 4, no. 8, pp. 2826–2830, 2011, doi: 10.1039/c1ee01198g.
- [30] R. Kumar *et al.*, “Fabrication and electrochemical evaluation of micro-supercapacitors prepared by direct laser writing on free-standing graphite oxide paper,” *Energy*, vol. 179, pp. 676–684, 2019, doi: 10.1016/j.energy.2019.05.032.
- [31] N. Devi, S. Sahoo, R. Kumar, and R. K. Singh, “A review of the microwave-assisted synthesis of carbon nanomaterials, metal oxides/hydroxides and their composites for energy storage applications,” *Nanoscale*, vol. 13, no. 27, pp. 11679–11711, 2021, doi: 10.1039/d1nr01134k.
- [32] I. Shown, A. Ganguly, L. C. Chen, and K. H. Chen, “Conducting polymer-based flexible supercapacitor,” *Energy Sci. Eng.*, vol. 3, no. 1, pp. 2–26, 2015, doi: 10.1002/ese3.50.
- [33] I. J. Gómez, M. V. Sulleiro, D. Mantione, and N. Alegret, “Carbon nanomaterials embedded in conductive polymers: A state of the art,” *Polymers (Basel)*, vol. 13, no. 5, pp. 1–54, 2021, doi: 10.3390/polym13050745.
- [34] S. B. Brachetti-Sibaja *et al.*, “Cvd conditions for mwcnts production and their effects on the optical and electrical properties of ppy/mwcnts, pani/mwcnts nanocomposites by in situ electropolymerization,” *Polymers (Basel)*, vol. 13, no. 3, pp. 1–29, 2021, doi: 10.3390/polym13030351.
- [35] M. Beygisangchin, S. A. Rashid, S. Shafie, A. R. Sadrolhosseini, and H. N. Lim, “Preparations, properties, and applications of polyaniline and polyaniline thin films—a review,” *Polymers (Basel)*, vol. 13, no. 12, 2021, doi: 10.3390/polym13122003.
- [36] C. An, Y. Zhang, H. Guo, and Y. Wang, “Metal oxide-based supercapacitors: progress and prospectives,” *Nanoscale Adv.*, vol. 1, no. 12, pp. 4644–4658, 2019, doi: 10.1039/c9na00543a.
- [37] J. Hong *et al.*, “Solubility-Dependent NiMoO<sub>4</sub> Nanoarchitectures: Direct Correlation between Rationally Designed Structure and Electrochemical Pseudokinetics,” *ACS Appl. Mater. Interfaces*, vol. 8, no. 51, pp. 35227–35234, 2016, doi: 10.1021/acsami.6b11584.
- [38] M. I. Rafiq, X. Wang, T. Farid, J. Zhou, J. Tang, and W. Tang, “Carbonyl-enriched hierarchical carbon synergizes redox electrolyte for highly-efficient and stable supercapacitors,” *Chem. Commun.*, vol. 57, no. 30, pp. 3716–3719, 2021, doi: 10.1039/d0cc08432h.
- [39] T. Farid, M. I. Rafiq, A. Ali, and W. Tang, “Transforming wood as next-generation structural and functional materials for a sustainable future,” *EcoMat*, vol. 4, no. 1, pp. 1–48, 2022, doi: 10.1002/eom2.12154.
- [40] T. Farid, M. I. Rafiq, A. Ali, and W. Tang, “Transforming wood as next-generation structural and functional materials for a sustainable future,” *EcoMat*, vol. 4, no. 1, Jan. 2022, doi: 10.1002/eom2.12154.



- [41] T. Farid, Y. Wang, M. I. Rafiq, A. Ali, and W. Tang, “Porous Flexible Wood Scaffolds Designed for High-Performance Electrochemical Energy Storage,” *ACS Sustain. Chem. Eng.*, vol. 10, no. 21, pp. 7078–7090, 2022, doi: 10.1021/acssuschemeng.2c01108.
- [42] A. Kumar, T. Jyske, and M. Petrič, “Delignified Wood from Understanding the Hierarchically Aligned Cellulosic Structures to Creating Novel Functional Materials: A Review,” *Adv. Sustain. Syst.*, vol. 5, no. 5, 2021, doi: 10.1002/adsu.202000251.
- [43] J. Jose, V. Thomas, V. Vinod, R. Abraham, and S. Abraham, “Nanocellulose based functional materials for supercapacitor applications,” *J. Sci. Adv. Mater. Devices*, vol. 4, no. 3, pp. 333–340, 2019, doi: 10.1016/j.jsamd.2019.06.003.
- [44] M. Sethi, H. Bantawal, U. S. Shenoy, and D. K. Bhat, “Eco-friendly synthesis of porous graphene and its utilization as high performance supercapacitor electrode material,” *J. Alloys Compd.*, vol. 799, pp. 256–266, 2019, doi: 10.1016/j.jallcom.2019.05.302.
- [45] R. Vinodh, Y. Sasikumar, H. J. Kim, R. Atchudan, and M. Yi, “Chitin and chitosan based biopolymer derived electrode materials for supercapacitor applications: A critical review,” *J. Ind. Eng. Chem.*, vol. 104, pp. 155–171, 2021, doi: 10.1016/j.jiec.2021.08.019.
- [46] D. Zhao, Y. Zhu, W. Cheng, W. Chen, Y. Wu, and H. Yu, “Cellulose-Based Flexible Functional Materials for Emerging Intelligent Electronics,” *Adv. Mater.*, vol. 33, no. 28, pp. 1–18, 2021, doi: 10.1002/adma.202000619.
- [47] P. Tapsanit and J. Maitip, “Optical properties of freeze-dried partial delignified balsa wood,” *J. Phys. Conf. Ser.*, vol. 2431, no. 1, 2023, doi: 10.1088/1742-6596/2431/1/012001.
- [48] V. H. R. Souza, M. M. Oliveira, and A. J. G. Zarbin, “Bottom-up synthesis of graphene/polyaniline nanocomposites for flexible and transparent energy storage devices,” *J. Power Sources*, vol. 348, pp. 87–93, 2017, doi: 10.1016/j.jpowsour.2017.02.064.
- [49] Y. Li *et al.*, “Green synthesis of free standing cellulose/graphene oxide/polyaniline aerogel electrode for high-performance flexible all-solid-state supercapacitors,” *Nanomaterials*, vol. 10, no. 8, pp. 1–18, 2020, doi: 10.3390/nano10081546.
- [50] M. Ben Hadj Said *et al.*, “Synthesis and characterization of cellulose hydrogel/graphene oxide/polyaniline composite for high-performing supercapacitors,” *Int. J. Energy Res.*, vol. 46, no. 10, pp. 13844–13854, 2022, doi: 10.1002/er.8102.
- [51] S. Lyu *et al.*, “Nanocellulose supported hierarchical structured polyaniline/nanocarbon nanocomposite electrode: Via layer-by-layer assembly for green flexible supercapacitors,” *RSC Adv.*, vol. 9, no. 31, pp. 17824–17834, 2019, doi: 10.1039/c9ra02449b.
- [52] P. Dubey, P. H. Maheshwari, and S. Sundriyal, “Human Hair-Derived Porous Activated Carbon as an Efficient Matrix for Conductive Polypyrrole for Hybrid Supercapacitors,” *Energy and Fuels*, vol. 36, no. 21, pp. 13218–13228, 2022, doi: 10.1021/acs.energyfuels.2c01926.
- [53] N. R. Aswathy, S. A. Kumar, S. Mohanty, S. K. Nayak, and A. K. Palai, “Polyaniline/multi-walled carbon nanotubes filled biopolymer based flexible substrate electrodes for supercapacitor applications,” *J. Energy Storage*, vol. 35, no. September

- 2020, p. 102256, 2021, doi: 10.1016/j.est.2021.102256.
- [54] M. Khan, “美国科学院学报 Materials Chemistry A 材料化学 a,” *J. Mater. Chem. A*, vol. 6, no. 207890, p. 121, 2015, doi: 10.1039/x0xx00xxx.
- [55] M. Hou, Y. Hu, M. Xu, and B. Li, “Nanocellulose based flexible and highly conductive film and its application in supercapacitors,” *Cellulose*, vol. 27, no. 16, pp. 9457–9466, 2020, doi: 10.1007/s10570-020-03420-2.
- [56] Y. Ruan, C. Wang, and J. Jiang, “Nanostructured Ni compounds as electrode materials towards high-performance electrochemical capacitors,” *J. Mater. Chem. A*, vol. 4, no. 38, pp. 14509–14538, 2016, doi: 10.1039/c6ta05104a.
- [57] C. Wang *et al.*, “ $\beta$ -NiMoO<sub>4</sub> nanowire arrays grown on carbon cloth for 3D solid asymmetry supercapacitors,” *RSC Adv.*, vol. 5, no. 129, pp. 107098–107104, 2015, doi: 10.1039/c5ra14704b.
- [58] H. Wang, J. Lin, and Z. X. Shen, “Polyaniline (PANi) based electrode materials for energy storage and conversion,” *J. Sci. Adv. Mater. Devices*, vol. 1, no. 3, pp. 225–255, 2016, doi: 10.1016/j.jsamd.2016.08.001.
- [59] Y. Han and L. Dai, “Conducting Polymers for Flexible Supercapacitors,” *Macromol. Chem. Phys.*, vol. 220, no. 3, pp. 1–14, 2019, doi: 10.1002/macp.201800355.
- [60] C. Pan, H. Gu, and L. Dong, “Synthesis and electrochemical performance of polyaniline @MnO<sub>2</sub>/graphene ternary composites for electrochemical supercapacitors,” *J. Power Sources*, vol. 303, pp. 175–181, 2016, doi: 10.1016/j.jpowsour.2015.11.002.
- [61] D. Liu, H. Wang, P. Du, W. Wei, Q. Wang, and P. Liu, “Flexible and robust reduced graphene oxide/carbon nanoparticles/polyaniline (RGO/CNs/PANI) composite films: Excellent candidates as free-standing electrodes for high-performance supercapacitors,” *Electrochim. Acta*, vol. 259, pp. 161–169, 2018, doi: 10.1016/j.electacta.2017.10.165.
- [62] S. Ahmed, A. Ahmed, and M. Rafat, “Supercapacitor performance of activated carbon derived from rotten carrot in aqueous, organic and ionic liquid based electrolytes,” *J. Saudi Chem. Soc.*, vol. 22, no. 8, pp. 993–1002, 2018, doi: 10.1016/j.jscs.2018.03.002.
- [63] Y. Yan, P. Gu, S. Zheng, M. Zheng, H. Pang, and H. Xue, “Facile synthesis of an accordion-like Ni-MOF superstructure for high-performance flexible supercapacitors,” *J. Mater. Chem. A*, vol. 4, no. 48, pp. 19078–19085, 2016, doi: 10.1039/c6ta08331e.
- [64] R. K. Mishra, M. H. Nawaz, A. Hayat, M. A. H. Nawaz, V. Sharma, and J. L. Marty, “Electrospinning of graphene-oxide onto screen printed electrodes for heavy metal biosensor,” *Sensors Actuators, B Chem.*, vol. 247, pp. 366–373, 2017, doi: 10.1016/j.snb.2017.03.059.
- [65] J. Song *et al.*, “Superflexible Wood,” *ACS Appl. Mater. Interfaces*, vol. 9, no. 28, pp. 23520–23527, 2017, doi: 10.1021/acsami.7b06529.
- [66] R. Vanholme, B. Demedts, K. Morreel, J. Ralph, and W. Boerjan, “Lignin biosynthesis and structure,” *Plant Physiol.*, vol. 153, no. 3, pp. 895–905, 2010, doi:

10.1104/pp.110.155119.

- [67] Y. Meng, J. Majoinen, B. Zhao, and O. J. Rojas, “Form-stable phase change materials from mesoporous balsa after selective removal of lignin,” *Compos. Part B Eng.*, vol. 199, no. February, p. 108296, 2020, doi: 10.1016/j.compositesb.2020.108296.
- [68] M. Taha, M. Hassan, S. Essa, and Y. Tartor, “Use of Fourier transform infrared spectroscopy (FTIR) spectroscopy for rapid and accurate identification of Yeasts isolated from human and animals,” *Int. J. Vet. Sci. Med.*, vol. 1, no. 1, pp. 15–20, 2013, doi: 10.1016/j.ijvsm.2013.03.001.
- [69] E. Y. Choi *et al.*, “Noncovalent functionalization of graphene with end-functional polymers,” *J. Mater. Chem.*, vol. 20, no. 10, pp. 1907–1912, 2010, doi: 10.1039/b919074k.
- [70] X. T. Tran, S. S. Park, S. Song, and M. S. Haider, “materials Electroconductive performance of polypyrrole / reduced graphene oxide / carbon nanotube composites synthesized via in situ oxidative polymerization,” *J. Mater. Sci.*, vol. 54, no. 4, pp. 3156–3173, 2019, doi: 10.1007/s10853-018-3043-4.
- [71] A. T. Habte, D. W. Ayele, and M. Hu, “Synthesis and Characterization of Reduced Graphene Oxide (rGO) Started from Graphene Oxide (GO) Using the Tour Method with Different Parameters,” *Adv. Mater. Sci. Eng.*, vol. 2019, no. Vc, 2019, doi: 10.1155/2019/5058163.
- [72] S. H. Ryu and A. M. Shanmugaraj, “Influence of long-chain alkylamine-modified graphene oxide on the crystallization, mechanical and electrical properties of isotactic polypropylene nanocomposites,” *Chem. Eng. J.*, vol. 244, pp. 552–560, 2014, doi: 10.1016/j.cej.2014.01.101.
- [73] N. Cao and Y. Zhang, “Study of Reduced Graphene Oxide Preparation by Hummers’ Method and Related Characterization,” *J. Nanomater.*, vol. 2015, pp. 1–5, 2015, doi: 10.1155/2015/168125.
- [74] K. K. Pandey, “A Study of Chemical Structure of Soft and Hardwood and Wood Polymers by FTIR Spectroscopy,” *J. Appl. Polym. Sci.*, vol. 71, no. 12, pp. 1969–1975, 1999, doi: 10.1002/(sici)1097-4628(19990321)71:12<1969::aid-app6>3.0.co;2-d.
- [75] C. Xiong *et al.*, “Non-carbonized porous lignin-free wood as an effective scaffold to fabricate lignin-free Wood@Polyaniline supercapacitor material for renewable energy storage application,” *J. Power Sources*, vol. 471, Sep. 2020, doi: 10.1016/j.jpowsour.2020.228448.
- [76] C. Yang *et al.*, “Flexible highly specific capacitance aerogel electrodes based on cellulose nanofibers, carbon nanotubes and polyaniline,” *Electrochim. Acta*, vol. 182, pp. 264–271, 2015, doi: 10.1016/j.electacta.2015.09.096.
- [77] C. Yang and D. Li, “Flexible and foldable supercapacitor electrodes from the porous 3D network of cellulose nanofibers, carbon nanotubes and polyaniline,” *Mater. Lett.*, vol. 155, pp. 78–81, 2015, doi: 10.1016/j.matlet.2015.04.096.
- [78] N. Elgrishi, K. J. Rountree, B. D. McCarthy, E. S. Rountree, T. T. Eisenhart, and J. L.

- Dempsey, "A Practical Beginner's Guide to Cyclic Voltammetry," *J. Chem. Educ.*, vol. 95, no. 2, pp. 197–206, 2018, doi: 10.1021/acs.jchemed.7b00361.
- [79] Y. Chang, G. Han, J. Yuan, D. Fu, F. Liu, and S. Li, "Using hydroxylamine as a reducer to prepare N-doped graphene hydrogels used in high-performance energy storage," *J. Power Sources*, vol. 238, pp. 492–500, 2013, doi: 10.1016/j.jpowsour.2013.04.074.
- [80] J. Yu *et al.*, "Flexible metallic fabric supercapacitor based on graphene/polyaniline composites," *Electrochim. Acta*, vol. 259, pp. 968–974, 2018, doi: 10.1016/j.electacta.2017.11.008.
- [81] H. Zhou, G. Han, Y. Xiao, Y. Chang, and H. J. Zhai, "Facile preparation of polypyrrole/graphene oxide nanocomposites with large areal capacitance using electrochemical codeposition for supercapacitors," *J. Power Sources*, vol. 263, pp. 259–267, 2014, doi: 10.1016/j.jpowsour.2014.04.039.
- [82] M. Ates and Y. Yuruk, "Facile preparation of reduced graphene oxide, polypyrrole, carbon black, and polyvinyl alcohol nanocomposite by electrospinning: a low-cost and sustainable approach for supercapacitor application," *Ionics (Kiel)*, vol. 27, no. 6, pp. 2659–2672, 2021, doi: 10.1007/s11581-021-04007-y.
- [83] J. Yan, J. Liu, Z. Fan, T. Wei, and L. Zhang, "High-performance supercapacitor electrodes based on highly corrugated graphene sheets," *Carbon N. Y.*, vol. 50, no. 6, pp. 2179–2188, 2012, doi: 10.1016/j.carbon.2012.01.028.
- [84] T. Fan *et al.*, "Self-assembling sulfonated graphene/polyaniline nanocomposite paper for high performance supercapacitor," *Synth. Met.*, vol. 199, pp. 79–86, 2015, doi: 10.1016/j.synthmet.2014.11.017.
- [85] R. Teimuri-Mofrad, E. Payami, and I. Ahadzadeh, "Synthesis, characterization and electrochemical evaluation of a novel high performance GO-Fc/PANI nanocomposite for supercapacitor applications," *Electrochim. Acta*, vol. 321, p. 134706, 2019, doi: 10.1016/j.electacta.2019.134706.
- [86] Z. S. Wu, Z. Liu, K. Parvez, X. Feng, and K. Müllen, "Ultrathin Printable Graphene Supercapacitors with AC Line-Filtering Performance," *Adv. Mater.*, vol. 27, no. 24, pp. 3669–3675, 2015, doi: 10.1002/adma.201501208.
- [87] A. Hodaei, A. S. Dezfouli, and H. R. Naderi, "A high-performance supercapacitor based on N-doped TiO<sub>2</sub> nanoparticles," *J. Mater. Sci. Mater. Electron.*, vol. 29, no. 17, pp. 14596–14604, 2018, doi: 10.1007/s10854-018-9595-x.
- [88] I. Y. Y. Bu and R. Huang, "Fabrication of CuO-decorated reduced graphene oxide nanosheets for supercapacitor applications," *Ceram. Int.*, vol. 43, no. 1, pp. 45–50, 2017, doi: 10.1016/j.ceramint.2016.08.136.
- [89] G. Zhang, T. Wang, X. Yu, H. Zhang, H. Duan, and B. Lu, "Nanoforest of hierarchical Co<sub>3</sub>O<sub>4</sub>@NiCo<sub>2</sub>O<sub>4</sub> nanowire arrays for high-performance supercapacitors," *Nano Energy*, vol. 2, no. 5, pp. 586–594, 2013, doi: 10.1016/j.nanoen.2013.07.008.